Ceramics International 47 (2021) 4972–4993

Contents lists available at ScienceDirect

Ceramics International

journal homepage: www.elsevier.com/locate/ceramint

Standardized Weibull statistics of ceramic strength

Wei-Sheng Lei [a,*], Zhishui Yu [a,**], Peilei Zhang [a,***], Guian Qian [b,****]

[a] School of Materials Engineering, Shanghai University of Engineering Science, Shanghai, 201620, China
[b] Institute of Mechanics, Chinese Academy of Sciences, Beijing, 100190, China

ARTICLE INFO

Keywords:
Ceramic strength
Statistical Weibull fracture theory
Ordinary Weibull distribution
Standardized Weibull distribution
Maximum likelihood estimation

ABSTRACT

In order to estimate Weibull parameters in the Weibull statistical fracture theory as truly material properties independent of specimen geometry and loading mode, first the Weibull statistical fracture theory is transformed into the ordinary Weibull distribution function under certain approximation. Then the standardized format of ordinary Weibull distribution is introduced to enable Weibull modulus as the single parameter for estimation via the maximum likelihood method. The method of using standardized Weibull distribution for strength data synchronization and Weibull modulus estimation is validated by analyzing extensive strength data sets measured from uniaxial flexure, biaxial flexure and their combination, and from smooth and notched specimens. The technical path to estimate the scale parameter and threshold strength as material properties in the Weibull statistical fracture theory and effect of sample size on the estimation accuracy are also discussed.

1. Introduction

Similar to other quasi-brittle materials such as rock, coal, wood, and concrete [1], the strength of ceramics is characterized by large random variation and strong specimen size effect. Both the empirical data fitting approach and the weakest link statistics have been adopted for statistical assessment of ceramic strength. The empirical data fitting approach adopts a variety of classical ordinary distribution functions to describe the statistical distribution of strength. For example, the ordinary Weibull distribution function [2], the normal distribution function, the log-normal distribution function and the Gamma distribution function are all used in Ref. [3] for characterization of ceramic strength. Overall, the ordinary Weibull distribution function is most commonly used for ceramics, with relevant industrial standards on calibration procedures being implemented, e.g., the ASTM standard C1239-00. As emphasized in Ref. [4,5], one downside is that the empirical data fitting approach cannot account for the specimen size effect on strength. It works well for strength data collected from a group of nominally same-sized specimens under a same loading condition. As specimen size or loading condition changes, empirical data fitting will be applied for each group of test. The size effect is reflected on the variation of the fitted distribution parameters with specimen size. However, since it is not based on physical understanding of fracture processes, the obtained empirical fitting formulae do not have prediction power for other different-sized specimens. Microscopically, the random variation of strength is believed to be due to the randomly distributed microdefects commonly existing in quasi-brittle materials in terms of spatial location, orientation, size and shape. This justifies the development of the probabilistic approaches, particularly the weakest link postulate-based statistical models to enable the prediction of effects of specimen size and loading condition on strength. The Weibull statistical fracture theory [6] falls into this category. As reported in Ref. [7], when different probability distribution functions are adopted to describe the statistical distribution of microcracks in a solid with respect to their strength or size, the corresponding weakest link models of the cumulative failure probability can be obtained with different complexity. Specific to ceramic materials, the Weibull statistical fracture theory [6] is the most commonly used weakest link statistical model. In literature, the term Weibull statistics refers to either the ordinary Weibull distribution function [2] or the Weibull statistical fracture theory [6]. While the mathematical formulations of the ordinary Weibull distribution function and the Weibull statistical fracture theory are somewhat similar, Lei et al. [5] emphasized their difference. The Weibull statistical fracture theory depends on the specific microscopic fracture criterion for arbitrary multiaxial

* Corresponding author.
** Corresponding author.
*** Corresponding author.
**** Corresponding author.
E-mail addresses: leiws2008@gmail.com (W.-S. Lei), yu_zhishui@163.com (Z. Yu), peilei@sues.edu.cn (P. Zhang), qianguian@imech.ac.cn (G. Qian).

https://doi.org/10.1016/j.ceramint.2020.10.073
Received 9 September 2020; Received in revised form 10 October 2020; Accepted 12 October 2020
Available online 13 October 2020

tensile/compressive stress states. Under the simplest maximum tensile principal stress criterion for fracture $\sigma_1 = \sigma \geq S$, the Weibull statistical fracture theory is expressed as

$$P(\sigma_N) = 1 - \exp\left[- \int_V \left(\frac{\sigma_1 - \sigma_{L,u}}{\sigma_u} \right)^{m_u} \frac{dV}{V_0} \right] \quad (\sigma_{L,u} \leq \sigma_1 < \infty) \tag{1}$$

where σ_1 is the maximum principal tensile stress component acting on a microcrack surface, S is the microscopic fracture strength; $\sigma_{L,u}$, σ_u, and m_u are the threshold strength, the scale parameter and the modulus in sequence, which are all material properties independent of specimen geometry (configuration and size) and loading mode; V_0 is a reference volume, dV *is* a differential volume element.

The ordinary Weibull distribution is an empirical distribution function on an equal footing with other classical ordinary distributions such as normal and Gamma distributions. It is used for a broad range of applications in engineering, geophysics, environmental science and ecology, medical science, social science and economics, such as deterioration rate of goods for inventory control [8] and insect population extrinsic mortality [9]. When it is applied to material strength, in isolation from specific microscopic fracture criterion, specimen geometry and loading mode, the ordinary Weibull distribution function simply describes the cumulative failure probability $P(\sigma_N)$ as a function of the nominal strength σ_N as below,

$$P(\sigma_N) = 1 - \exp\left[- \left(\frac{\sigma_N - \sigma_{L,0}}{\sigma_0} \right)^{m_0} \right] (\sigma_{L,0} \leq \sigma_N < \infty) \tag{2}$$

where $\sigma_{L,0}$, σ_0, and m_0 are all fitting parameters characterizing the threshold strength, the scale parameter and the modulus in sequence. Note that in Equations (1) and (2) we use two sets of parameters ($\sigma_{L,u}$, σ_u, m_u) and ($\sigma_{L,0}$, σ_0, m_0) to address the differences between the two statistical models.

Here we are faced with two important aspects of the ordinary Weibull distribution function. On the one hand, the dependency on specific microscopic fracture criterion differentiates the Weibull statistical fracture theory from the ordinary Weibull distribution function. For example, the maximum tensile principal stress criterion-based Weibull statistical fracture theory Equation (1) is invalid to evaluate ceramic strength in uniaxial compression but the ordinary Weibull distribution function works. Unlike the material parameters ($\sigma_{L,u}$, σ_u, m_u), the fitting parameters ($\sigma_{L,0}$, σ_0, m_0) vary with specimen geometry (configuration and size) and loading mode. So, the ordinary Weibull distribution function has no prediction power for the effects of specimen geometry and loading mode on the nominal strength σ_N. While on the other hand, thanks to its well established calibration procedures, the ordinary Weibull distribution function is more commonly adopted for ceramic strength evaluation than the Weibull statistical fracture theory. In view of the two aspects, this work explores a new approach to estimating the Weibull modulus m_u based on the ordinary Weibull distribution function, which will facilitate further estimation of the other two parameters ($\sigma_{L,u}$, σ_u) via other approaches. First, we demonstrate how to transform the formulation of Weibull statistical fracture theory into the format of the ordinary Weibull distribution function, which can be further approximately treated as the ordinary Weibull distribution function by assuming a constant value of a coefficient to the nominal stress σ_N. Second, the standardized expression of the ordinary Weibull distribution is presented, which has Weibull modulus as the single parameter. This standardized expression permits to synchronize multiple strength data sets measured on specimens of different geometry and size under different loading modes. Third, a plenty of ceramic strength data are adopted to prove the validity of using the standardized Weibull distribution function to estimate Weibull modulus. This is followed by a discussion on how to evaluate the remaining Weibull parameters in future studies.

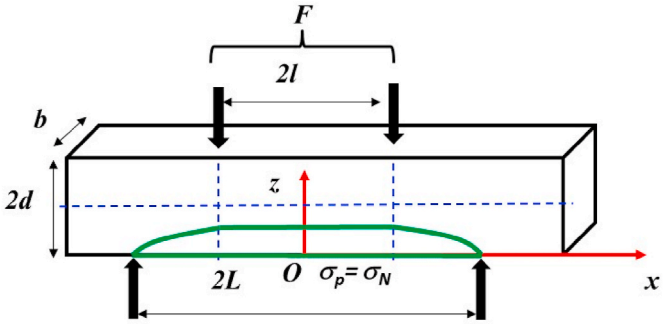

Fig. 1. A prismatic beam of rectangular cross section in four-point flexure.

2. Transformation of the Weibull statistical fracture theory to the ordinary Weibull distribution function

In an elastic material (e.g. ceramics) under arbitrary loading conditions, the maximum principal tensile stress σ_1 can be expressed as

$$\sigma_1 = \sigma_N \cdot f(x, y, z) \tag{3}$$

where $f(x,y,z)$ is a function of the coordinates (x,y,z) and loading mode. Thus, Equation (1) reduces to

$$P(\sigma_N) = 1 - \exp\left\{ - \int_V \left[\frac{\sigma_N \cdot f(x,y,z) - \sigma_{L,u}}{\sigma_u} \right]^{m_u} \frac{dV}{V_0} \right\} \quad (\sigma_{L,u} \leq \sigma_1 < \infty) \tag{4}$$

According to the mean value theorem for integrals that a continuous function on a closed, bounded interval has at least one point $\xi(x_\xi, y_\xi, z_\xi)$ where the function is equal to its average value on the interval, Equation (4) is rewritten as:

$$1 - P(\sigma_N) = \exp\left[- \left(\frac{k \cdot \sigma_N - \sigma_{L,u}}{\sigma_u} \right)^{m_u} \cdot \frac{V}{V_0} \right] = \exp\left\{ - \left[\underbrace{\frac{\sigma_N - \overbrace{\sigma_{L,u}/k}^{\sigma_{L,0}}}{\left(\sigma_u/k\right) \cdot (V_0/V)^{1/m_u}}}_{\sigma_0} \right]^{m_u} \right\} \tag{5}$$

Note that here the coefficient $k = f(x_\xi, y_\xi, z_\xi)$ is not a constant but varies with the ratio $\sigma_{L,u}/\sigma_N$ and loading mode, which can be explained by the example of uniaxial flexure. Fig. 1 schematically illustrates a prismatic beam of rectangular cross section in a four-point flexure setup, where 2 d is the specimen thickness, b is the specimen width, *2L* is the support span, 2*l* is the loading span, respectively, z and x are the distances from point O as the boundary line of peak stress σ_p in the thickness and length directions, respectively. The peak stress is taken as the nominal stress, $\sigma_N = \sigma_p$. The fracture process zone (FPZ) in which $\sigma_{L,u} \leq \sigma(x,z) \leq \sigma_N$ is satisfied is schematically shown by the area surrounded by the green line. As $l = 0$, the four-point flexure reduces to the three-point flexure. The tensile stress distribution in a three-point flexure follows,

$$\sigma(x,z) = \sigma_N (1 - z/d)(1 - |x|/L) (-L \leq x \leq L,\ 0 \leq z \leq d) \tag{6}$$

For the three-point flexure ($l = 0$), the fracture process zone (FPZ) reduces to a semi-elliptical shaped area defined by

$$0 \leq z \leq d \cdot \left(1 - \frac{\sigma_{L,u}}{\sigma_N}\right), \quad 0 \leq |x| \leq L \cdot \left[1 - \frac{\sigma_{L,u}}{\sigma_N (1 - z/d)}\right] \tag{7a, b}$$

The volume of FPZ conforming to (7a,b) is

$$V_{FPZ} = 2b \int_0^{d\cdot\left(1-\sigma_{L,u}/\sigma_N\right)} dz \int_0^{L\cdot\left[1-\frac{\sigma_{L,u}}{\sigma_N(1-z/d)}\right]} dx = V \cdot \left[1 - \frac{\sigma_{L,u}}{\sigma_N} + \frac{\sigma_{L,u}}{\sigma_N} ln\left(\frac{\sigma_{L,u}}{\sigma_N}\right)\right] \tag{8}$$

where $V = 2bLd$ is half specimen volume in tension. The specific point $\xi(x_\xi, y_\xi = b, z_\xi)$ that satisfies Equation (5) is confined within FPZ defined by (7a,b). As shown in Appendix A, k as a function of the ratio $\sigma_{L,u}/\sigma_N$ is given by

$$k = \frac{\sigma_{L,u}}{\sigma_N} + \left\{ \frac{1}{(m_u+1)} Ln\left(\frac{\sigma_{L,u}}{\sigma_N}\right) \left[\frac{1}{(1-\xi)} \frac{\sigma_{L,u}}{\sigma_N} - 1 \right]^{m_u+1} \right\}^{\frac{1}{m_u}} \tag{9}$$

where ξ is a constant and $0 \le \xi \le 1 - \sigma_{L,u}/\sigma_N \le 1$. There is $0 \le k \le 1$ for $\sigma_{L,u} \le \sigma_N < \infty$.

In addition, the Weibull statistical fracture theory in Equation (1) assumes a uniform spatial distribution of flaws in a material, i.e., the number of flaws in a volume V is proportional to V. The spatial distribution of flaws in a material also can be non-uniform. In the case that the number of flaws in a volume V is a power function of V, Lei [1] obtained the generalized Weibull statistical fracture theory:

$$P = 1 - \exp\left[-\beta \left(\frac{V}{V_0}\right)^{\beta-1} \int_V \left(\frac{\sigma_1 - \sigma_{L,u}}{\sigma_u}\right)^{m_u} \frac{dV}{V_0} \right] \tag{10}$$

where β is a material constant with $\beta > 0$ that describes the number (N) of flaws in a volume V by $N = (V/V_0)^\beta$. When $\beta = 1$, Equation (10) reduces to Equation (1). Equation (10) has been validated by strength data of ceramics and other quasi-brittle materials including concrete and intermetallic compounds [1,4,10,11].

The mean value theorem for integrals permits to rewrite Equation (10) as:

$$\begin{aligned} 1 - P(\sigma_N) &= \exp\left[-\beta \cdot \left(\frac{k\cdot\sigma_N - \sigma_{L,u}}{\sigma_u}\right)^{m_u} \cdot \left(\frac{V}{V_0}\right)^{\beta} \right] \\ &= \exp\left\{ - \left[\frac{\sigma_N - \overbrace{(\sigma_{L,u}/k)}^{\sigma_{L,0}}}{\underbrace{(\sigma_u/k)\cdot(1/\beta)^{1/m_u}\cdot(V_0/V)^{\beta/m_u}}_{\sigma_0}} \right]^{m_u} \right\} \end{aligned} \tag{11}$$

It is complicate to calibrate the multiple model parameters in Equations (5) and (11). One way is to first estimate the most important parameter, Weibull modulus m_u. This will significantly reduce the difficulty to further estimate the other material parameters $\sigma_{L,u}$, σ_u, and β. Now the question is: For different specimen configurations and loading modes, can we approximately assume that the coefficient k is independent of $\sigma_{L,u}/\sigma_N$ but still varies with specimen geometry and loading mode? If this assumption is acceptable, it is feasible to estimate Weibull modulus m_u by Equation (2) for the ordinary Weibull distribution function with:

$$m_0 = m_u, \quad \sigma_{L,0} = \sigma_{L,u}/k, \quad \sigma_0 = (\sigma_u/k)\cdot(V_0/V)^{1/m_0} \tag{12}$$

for Equation (5) and

$$m_0 = m_u, \quad \sigma_{L,0} = \sigma_{L,u}/k, \quad \sigma_0 = (\sigma_u/k)\cdot(V_0/V)^{\beta/m_0}\cdot(1/\beta)^{1/m_0} \tag{13}$$

for Equation (11).

Equations (5) and (11)–(13) apply to arbitrary loading conditions and can be simplified under additional conditions. For example, with $\sigma_{L,u} = 0$, there are

$$k = \left[\int_V \left(\frac{\sigma_1}{\sigma_N}\right)^{m_0} \frac{dV}{V} \right]^{1/m_0} \tag{14}$$

$$m_0 = m_u, \quad \sigma_{L,0} = \sigma_{L,u} = 0, \quad \sigma_0 = (\sigma_u/k)\cdot(V_0/V)^{1/m_0} \tag{15}$$

Note that a consensus is yet available on a zero-valued threshold fracture strength ($\sigma_{L,u} = 0$) for ceramics [5,12,13]. In fact, The adoption of two-parameter Weibull statistical fracture model is often at a cost of the dependence of Weibull parameters (m_u , σ_u) on stress states and effective specimen volume governed by specimen geometry and loading mode [14–16]. This is against the basic assumption of Weibull statistical fracture theory on initial flaw distribution prior to loading, making the Weibull prediction problematic [16].

In plain uniaxial tension ($\sigma_1 = \sigma_N$), there is

$$k = 1, \quad m_0 = m_u, \quad \sigma_{L,0} = \sigma_{L,u}, \quad \sigma_0 = \sigma_u\cdot(V_0/V)^{1/m_0} \tag{16}$$

3. The standardized Weibull distribution function

3.1. Standardization process

The ordinary Weibull distribution has its cumulative distribution function (CDF) described by Equation (2), while its probability density function (PDF) is given as

$$\text{PDF: } f(x,\ m, x_L, x_0\ ) = \frac{m_0}{\sigma_0}\left(\frac{\sigma_N - \sigma_{L,0}}{\sigma_0}\right)^{m_0-1} exp\left[-\left(\frac{\sigma_N - \sigma_{L,0}}{\sigma_0}\right)^{m_0} \right] \tag{17}$$

The population mean (μ_{σ_N}), standard deviation (δ_{σ_N}), and excess kurtosis (γ_2) are:

$$\mu_{\sigma_N} = \sigma_{L,0} + \sigma_0\Gamma_1 \tag{18}$$

$$\delta_{\sigma_N} = \sigma_0\sqrt{\Gamma_2 - \Gamma_1^2} \tag{19}$$

$$\gamma_2 = \frac{-6\Gamma_1^4 + 12\Gamma_1^2\Gamma_2 - 3\Gamma_2^2 - 4\Gamma_1\Gamma_3 + \Gamma_4}{(\Gamma_2 - \Gamma_1^2)^2} \tag{20}$$

where $\Gamma(m_0) = \int_0^\infty e^{-x}x^{m_0-1}dx$ is the Gamma function, $\Gamma_i = \Gamma(1 + i/m_0)$, $i = 1, 2, 3, 4$.

Now we introduce the following new variable y as the standardized form of variable σ_N,

$$y = \frac{\sigma_N - \mu_{\sigma_N}}{\delta_{\sigma_N}} \quad \text{or} \quad \sigma_N = \mu_{\sigma_N} + y\cdot\delta_{\sigma_N} \tag{21}$$

There is

$$\frac{\sigma_N - \sigma_{L,0}}{\sigma_0} = \Gamma_1 + y\cdot\sqrt{\Gamma_2 - \Gamma_1^2} \tag{22}$$

Therefore, Equations (2) and (17) reduce to their standardized forms with a single parameter m_0

$$\text{CDF: } F\left(y = \frac{\sigma_N - \mu_{\sigma_N}}{\delta_{\sigma_N}}\right) = 1 - exp\left[-\left(\frac{y - y_L}{y_0}\right)^{m_0} \right] \ (y \ge y_L) \tag{23}$$

$$\text{PDF: } f\left(y = \frac{\sigma_N - \mu_{\sigma_N}}{\delta_{\sigma_N}}\right) = \frac{m_0}{y_0}\left(\frac{y - y_L}{y_0}\right)^{m_0-1} exp\left[-\left(\frac{y - y_L}{y_0}\right)^{m_0} \right] \ (y \ge y_L) \tag{24}$$

with

$$y_L = y_L(m_0) = -\frac{\Gamma_1}{\sqrt{\Gamma_2 - \Gamma_1^2}} \tag{25}$$

and

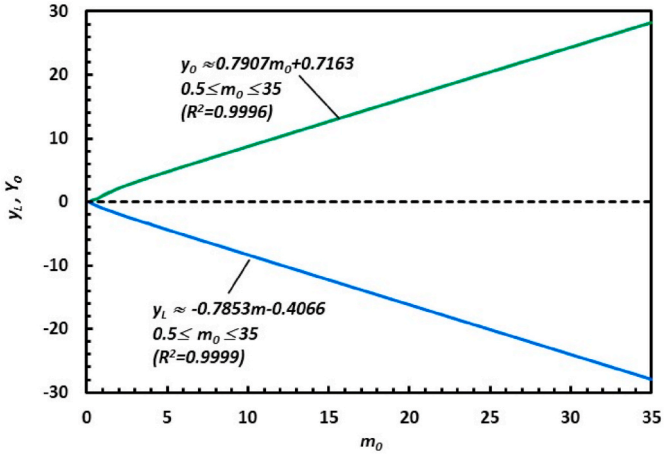

Fig. 2. Variations of parameters y_L and y_0 with m_0.

$$y_0 = y_0(m_0) = \frac{1}{\sqrt{\Gamma_2 - \Gamma_1^2}} \tag{26}$$

The standardized Weibull distribution remains same shape as Equation (2) but has its population average $\mu_y = 0$ and population standard deviation $\delta_y = 1$ due to

$$\mu_y = y_L + y_0\Gamma_1 = 0 \tag{27}$$

$$\delta_y = y_0\sqrt{\Gamma_2 - \Gamma_1^2} = 1 \tag{28}$$

Fig. 2 shows the variations of parameters y_L and y_0 with m_0 with the following linear approximations:

$$y_0 = 0.7907m_0 + 0.7163,\ 0.5 \le m_0 \le 35\ \left(R^2 = 0.9996\right) \tag{29}$$

$$y_L = -0.7853m_0 - 0.4066,\ 0.5 \le m_0 \le 35\ \left(R^2 = 0.9999\right) \tag{30}$$

3.2. Parameters estimation

3.2.1. Estimation of m_0

The population mean (μ_{σ_N}) and standard deviation (δ_{σ_N}) are estimated by sample mean ($\overline{\sigma_N}$) and standard deviation (s_{σ_N}) of the n sampled data

$$\widehat{\mu}_{\sigma_N} = \overline{\sigma}_N = \frac{\sum_{i=1}^{n}\sigma_{N,i}}{n} \tag{31}$$

and

$$\widehat{\delta}_{\sigma_N} = s_{\sigma_N} = \sqrt{\frac{\sum_{i=1}^{n}\left(\sigma_{N,i} - \overline{\sigma}_N\right)^2}{n - 1.5 - 0.25\gamma_2}} \tag{32}$$

where γ_2 denotes the population excess kurtosis, $\sigma_{N,i}$ is the i-th data point of nominal strength of n nominal strength measurements ranked in an ascending order ($i = 1, 2, \ldots, n$). For Weibull distribution with a modulus m_0, γ_2 is defined in Equation (20). Equations (31) is an unbiased estimator of μ_{σ_N}. Equation (32) is an approximate formula for the unbiased estimator of δ_{σ_N} for non-normal distributions [17]. The common expression for sample standard deviation is a biased estimator of δ_{σ_N}:

$$\widehat{\delta}_{\sigma_N} = s_{\sigma_N} = \sqrt{\frac{\sum_{i=1}^{n}\left(\sigma_{N,i} - \overline{\sigma}_N\right)^2}{(n-1)}} \tag{33}$$

Equation (32) is inconvenient to use. The following approximation is adopted instead:

$$\widehat{\delta}_{\sigma_N} = s_{\sigma_N} = \sqrt{\frac{\sum_{i=1}^{n}\left(\sigma_{N,i} - \overline{\sigma}_N\right)^2}{(n-1.5)}} \tag{34}$$

For $1.5 \le m_0 \le 20.5$, there is $-0.29 \le \gamma_2 \le 1.39$. Within this range,

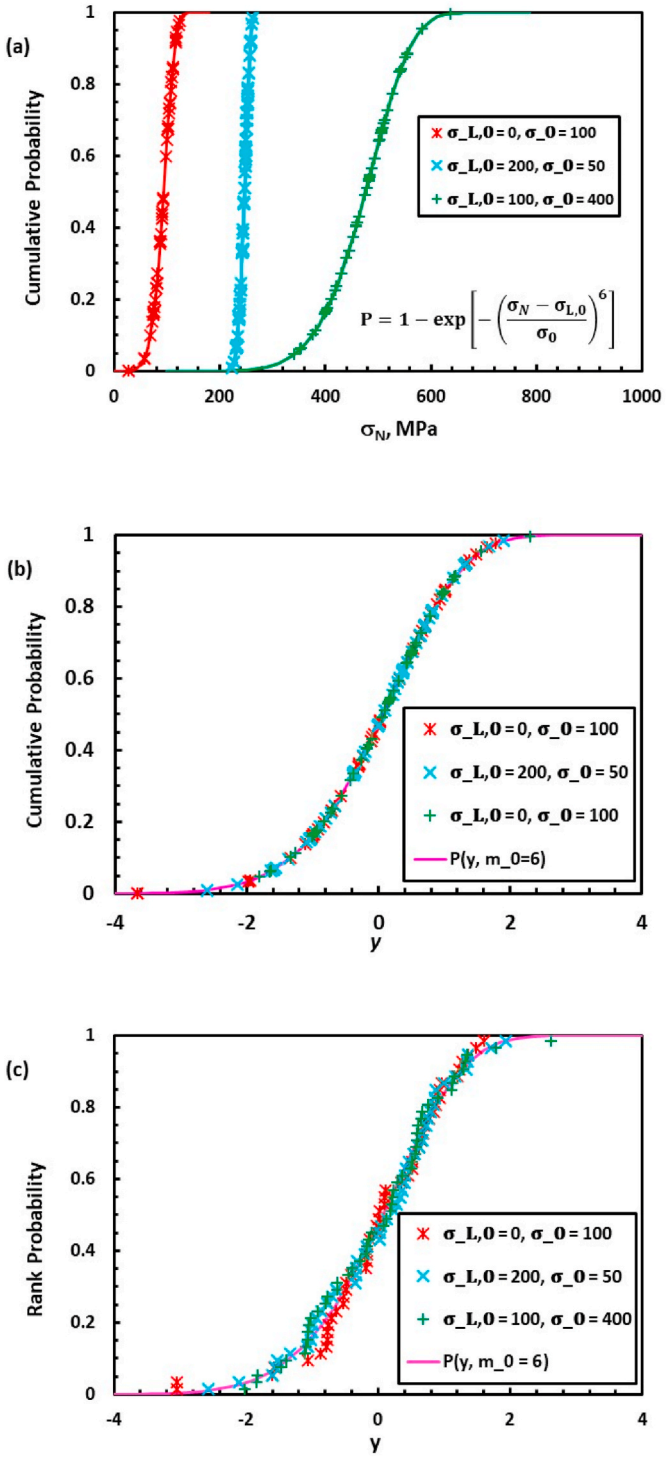

Fig. 3. Three strength distributions all with $m_0 = 6$ but different σ_0 and $\sigma_{L,0}$ in ordinary format **(a)** and in standardized formats **(b)** with exact cumulative probability and population mean and standard deviation, and **(c)** with rank probability and sample mean and standard deviation.

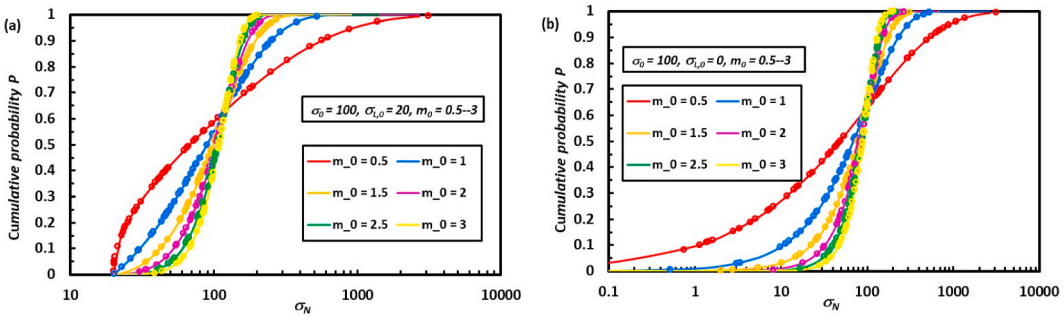

Fig. 4. Ordinary Weibull distributions and 50 samples on each distribution with $\sigma_{L,0} = 20, \sigma_0 = 100$ but different m_0 in scenario (1) **(a)** and $\sigma_{L,0} = 20, \sigma_0 = 100$ but different m_0 in scenario (2) **(b)**.

the difference in the value of $\widehat{\delta}_{\sigma_N}$ is 0.4–2.1% between Equation (32) and Equation (34) with sample number $n = 10$ and reduces to 0.19–0.95% with sample number $n = 20$.

The sampled data $\sigma_{N,i}$ $(i = 1, 2, \ldots, n)$ are converted into standardized values y_i $(i = 1, 2, \ldots, n)$

$$y_i = \frac{\sigma_{N,i} - \widehat{\mu}_{\sigma_N}}{s_{\sigma_N}} \quad (i = 1, 2, \ldots n) \tag{35}$$

The data set y_i $(i = 1, 2, \ldots, n)$ follows the standardized Weibull distribution in (23) and (24). m_0 is estimated by maximizing the logarithmic likelihood function with respect to m_0:

$$l(y_L,\ y_0, m_0) = nln\left(\frac{m_0}{y_0}\right) + (m_0 - 1)\sum_{i=1}^{n} \ln\left(\frac{y_i - y_L}{y_0}\right) - \sum_{i=1}^{n}\left(\frac{y_i - y_L}{y_0}\right)^{m_0} \tag{36}$$

Note that both y_L and y_0 are functions of m_0 as given in (27) and (28).

3.2.2. Estimation of $\boldsymbol{\sigma}_{L,0}$ and $\boldsymbol{\sigma}_0$

With the estimated value of m_0, $\widehat{m}_0$, as input, the remaining two parameters $\sigma_{L,0}$ and σ_0 are estimated by:

$$\widehat{\sigma}_0 = \frac{s_{\sigma_N}}{\sqrt{\Gamma_2 - \Gamma_1^2}} = y_0 \cdot S_{\sigma_N} \tag{37}$$

$$\widehat{\sigma}_{L,0} = \overline{\sigma}_N - \frac{\Gamma_1}{\sqrt{\Gamma_2 - \Gamma_1^2}} \cdot s_{\sigma_N} = \overline{\sigma}_N + y_L \cdot s_{\sigma_N} \tag{38}$$

3.2.3. The range of $\boldsymbol{m}_0$

The threshold value $\sigma_{L,0}$ of the nominal strength falls in the range below:

$$0 \le \sigma_{L,0} \le \sigma_{N,(1)} \tag{39}$$

where $\sigma_{N,(1)} = Min\{\sigma_{N,i}, i = 1, 2, ..i, .., n\}$ is the minimum value of the nominal strength measurements $(\sigma_{N,1}, \sigma_{N,2}, \ldots, \sigma_{N,i}, \ldots, \sigma_{N,n})$. Substituting

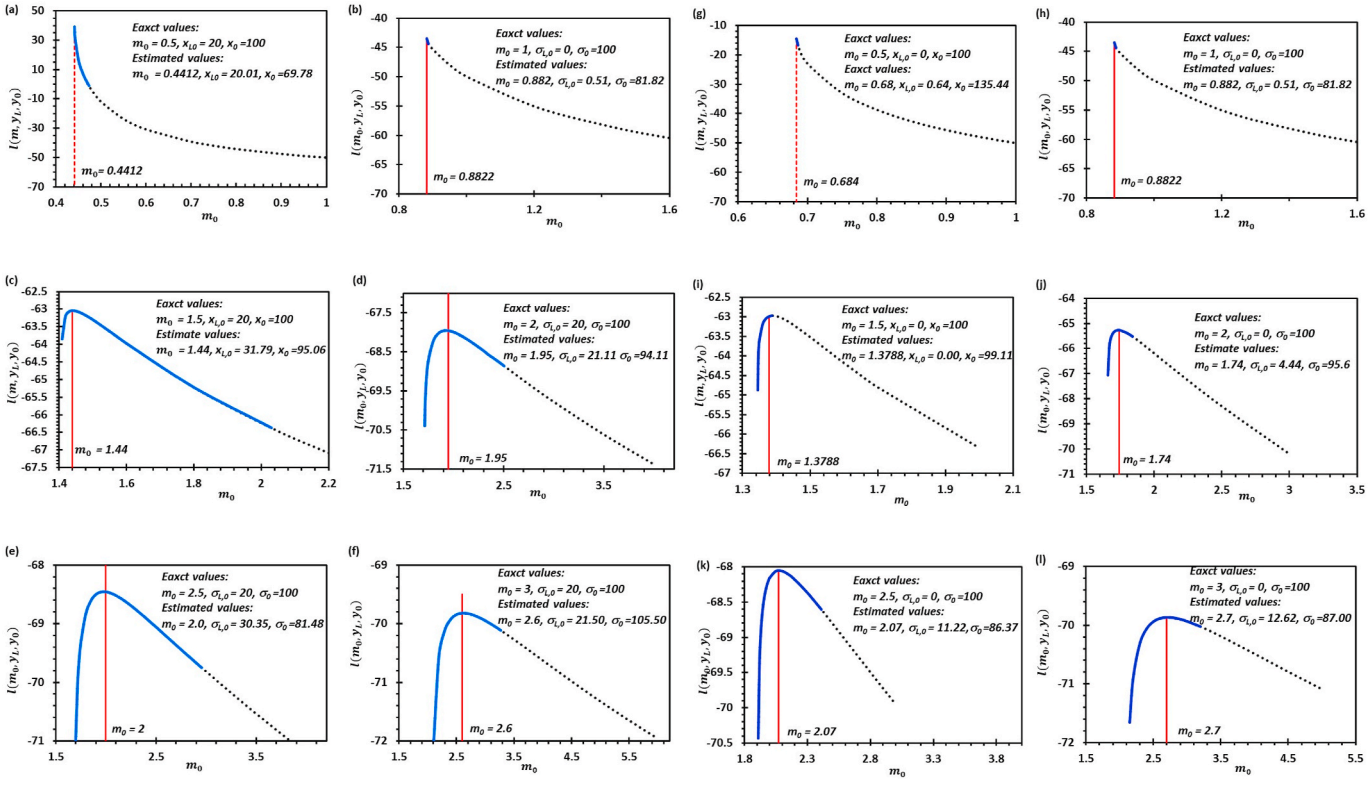

Fig. 5. Variation of log-likelihood function $l(m_0, y_L, y_0)$ with m_0 for scenarios (1) and (2).

Table 1
Summary of Weibull parameter estimation using different approaches.

Method of estimation		$\widehat{m}_0$	$\widehat{\sigma}_{L,0}$, MPa	$\widehat{\sigma}_0$, MPa	$\widehat{m}_u$	$\widehat{\sigma}_{L,u}$, MPa	$\widehat{\sigma}_u$, MPa
2-Parameter weibull distribution [3]	Maximum likelihood	9.05	0	305.54			
Master curve Equation (38) [5]	Least square				7.17	55	164.73
Standardized Weibull distribution Equation (mm)[This study]	Maximum likelihood	7.03	65.57	239.39			

Equation (38) in (39) yields:

$$0 \le \overline{\sigma}_N + y_L \cdot s_{\sigma_N} \le \sigma_{N,(1)} \tag{40}$$

or

$$-\frac{\overline{\sigma}_N}{s_{\sigma_N}} \le y_L \le \frac{\sigma_{N,(1)} - \overline{\sigma}_N}{s_{\sigma_N}} \tag{41}$$

Due to the monotonous correlation between y_L and m_0 as in Fig. 2, the range of m_0 is set by expression (41). When Equation (30) is adopted, (41) reduces to

$$1.2734\left(\frac{\overline{\sigma}_N - \sigma_{N,(1)}}{s_{\sigma_N}}\right) - 0.5178 \le m_0 \le 1.2734\left(\frac{\overline{\sigma}_N}{s_{\sigma_N}}\right) - 0.5178, \quad 0.5 \le m_0 \le 35 \tag{42}$$

The estimated value of m_0 must fall in this range to observe the inequality (41).

The key takeaway of Equations (23) and (24) is that for the ordinary Weibull distributions with an equal shape parameter m_0 but different values of $\sigma_{L,0}$ and σ_0, regardless of $\sigma_{L,0} = 0$ or $\sigma_{L,0} \neq 0$, they share the same standardized format with a single parameter m_0. This permits us to estimate m_0 with no need to know either $\sigma_{L,0} = 0$ or $\sigma_{L,0} \neq 0$ in advance.

As an example, Fig. 3 shows the following three Weibull distributions in their ordinary format **(a)** and standardized formats **(b)** and **(c)**, with

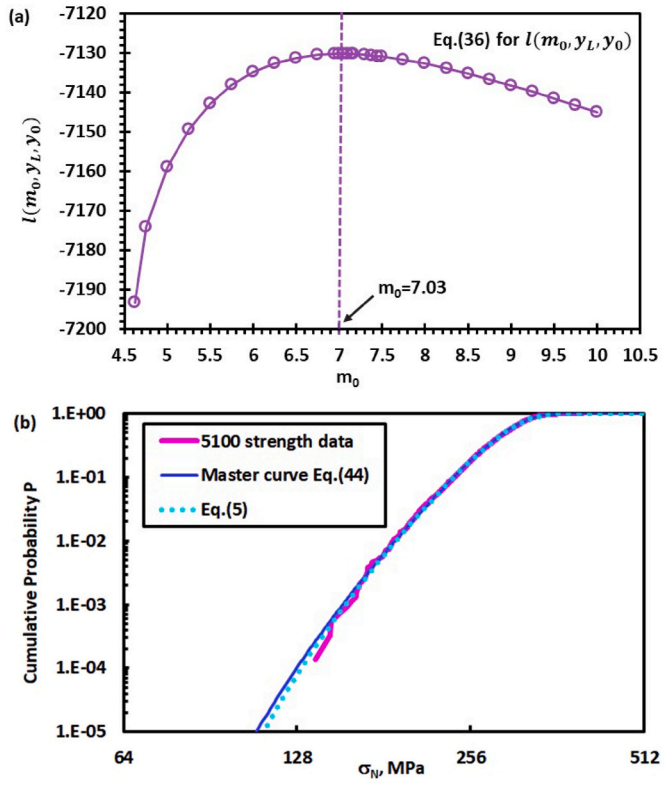

Fig. 6. Maximum likelihood estimation of m_0 **(a)** and comparison of predicted cumulative failure probability with experimental result **(b)**.

50 data points randomly generated on each distribution ($\sigma_{L,0}$ and σ_0 are in unit of MPa):

(1) . $m_0 = 6$, $\sigma_{L,0} = 0$, $\sigma_0 = 100$;
(2) . $m_0 = 6$, $\sigma_{L,0} = 200$, $\sigma_0 = 50$;
(3) . $m_0 = 6$, $\sigma_{L,0} = 100$, $\sigma_0 = 400$.

Note that in Fig. 3(b), the 50 standardized data points in each distribution are based on their known exact values of cumulative probability and population parameters (μ_{σ_N}, δ_{σ_N}) according to Equations (18) and (19). Therefore, all the three sets of data points fall exactly on the standardized distribution $P(y, m_0 = 6)$. While in Fig. 3(c), the 50 standardized data points in each distribution are based on their rank probabilities and sample average ($\overline{\sigma}_N$) and standard deviation (s_{σ_N}) according to Equations (31) and (34). As a result, all the three sets of data points approximately fall on the standardized distribution $P(y, m_0 = 6)$.

To gain a preliminary understanding of the accuracy of the proposed estimation method, we now consider 6 sets of three-parameter ordinary Weibull distributions of variable σ_N in two scenarios:

(1) All the distributions have $\sigma_{L,0} = 20, \sigma_0 = 100$ but $m_0 = 0.5, 1, 1.5, 2, 2.5, 3$, respectively;
(2) All the distributions have $\sigma_{L,0} = 0, \sigma_0 = 100$ but $m_0 = 0.5, 1, 1.5, 2, 2.5, 3$, respectively.

50 data points are randomly generated from each distribution in each scenario to serve as samples for maximum likelihood estimation of m_0 using Equation (36).

Fig. 4 (a) and **(b)** show the raw data for scenarios (1) and (2) in sequence. Fig. 5 (a)—(*l*) show the variation of log-likelihood function $l(m_0, y_{L,0}, y_0)$with m_0 for each distribution in Fig. 4. The dashed lines show the whole range of calculation, while the solid blue lines highlight the range of m_0 that satisfies inequality (42).

All these examples obtain close estimations of Weibull modulus m_0. More comprehensive investigation on the performance of the proposed approach will be investigated by Monte Carlo simulation as a separate study.

4. Applications to statistics of ceramic strength

As shown in Section 2, the statistical Weibull fracture theory reduces to Equation (5). While Equation (5) looks similar in format to the ordinary Weibull distribution function in Equation (2), it contains a coefficient $k = f(x_\xi, y_\xi, z_\xi)$ that varies with the ratio $\sigma_{L,u}/\sigma_N$ and loading mode rather than being a constant. In order to apply the standardized Weibull distribution to estimate Weibull modulus, we boldly assume that the coefficient k can be approximately treated as a constant independent of the ratio $\sigma_{L,u}/\sigma_N$ but still varies with loading mode. In this session, several case studies that cover uniaxial, biaxial, and triaxial stress states will be presented to evaluate this assumption and to demonstrate the potential applications of the standardized Weibull distribution for statistical evaluation of ceramic strength. Note that our focus here is to estimate $m_0 \approx m_u$. As shown in Equations (12) and (13), it takes additional efforts to transform the location and scale parameters ($\sigma_{L,0}$, σ_0) into material parameters ($\sigma_{L,u}$, σ_u). Specifically, the following aspects will be evaluated:

Table 2
Summary of flexural experiments of Al_2O_3 ceramics.

Data set #	Loading Mode	Specimen Cross-Section Size (mm)	Fixture, Support Span 2L, Loading Span 2*l* (mm)	Loading Rate, mm/min	Number of Specimens	Average, MPa	Standard Deviation, MPa	Laboratory & Operator
1	4PB	3 × 4	MIL STD B Fixture $2L = 40\ mm$; $2l = 20\ mm$	0.5	30	359	37	NPL (Morrell)
2					35	353	50	MRL (Johnston)
3					30	347	44	ORF (Sullivan)
4					32	364	45	ARE (Quinn)
5				2.0	30	323	52	ARE (Godfrey)
6				Unreported	33	381	32	IITRI (for AFWAL)
7			IITRI Modified Fixture $2L = 40\ mm$; $2l = 20\ mm$	Unreported	35	365	56	IITRI (for AFWAL)
8			NPL Fixture $2L = 40\ mm$; $2l = 20\ mm$	0.5	31	363	39	NPL (Morrell)
9			ARE Fixture $2L = 40\ mm$; $2l = 19.05\ mm$	2.0	30	378	39	ARE (Godfrey)
10		3 × 6	MIL STD B Fixture $2L = 40\ mm$; $2l = 20\ mm$	0.5	30	345	34	NPL (Morrell)
11					31	341	48	MTL (Quinn)
12				Unreported	35	362	33	IITRI (for AFWAL)
13		3.175 × 6.35 (1/8 × ¼ in.)	IITRI Fixture$2L = 44.45\ mm$ (1.750 in.); $2l = 22.225\ mm$(0.875 *in.*)	Unreported	35	343	49	IITRI (for AFWAL)
14		6 × 8	MIL STD C Fixture $2L = 80\ mm$;$2l = 40\ mm$	1.0	32	330	35	MTL (Quinn)
15		1.5 × 2	MIL STD A Fixture $2L = 20\ mm$;$2l = 10\ mm$	0.5	32	372	56	MTL (Quinn)
16	3PB	3 × 4	MIL STD B Fixture $2L = 40\ mm$	0.5	34	434	51	ORF (Sullivan)
17					30	444	51	MTL (Quinn)
18				2.0	10	400	25	ARE (Godfrey)
19			ARE Fixture $2L = 40\ mm$	2.0	30	452	63	ARE (Godfrey)

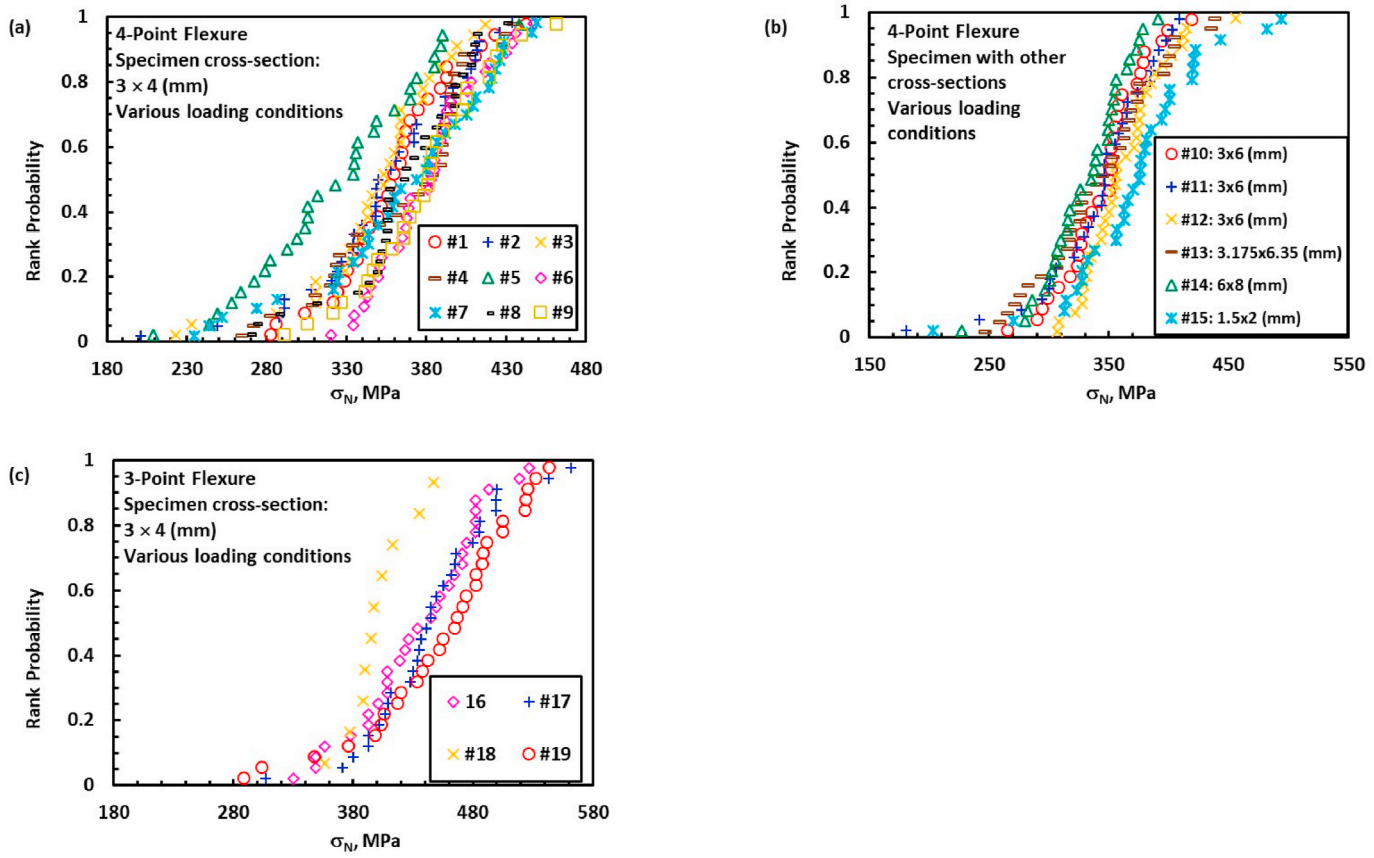

Fig. 7. Experimental strength data [18] of alumina measured by (a). four-point flexure of prismatic beams with cross section size of 3 mm × 4 mm; (b). four-point flexure of prismatic beams with other sized cross sections; (c). three-point flexure of prismatic beams with cross section size of 3 mm × 4 mm.

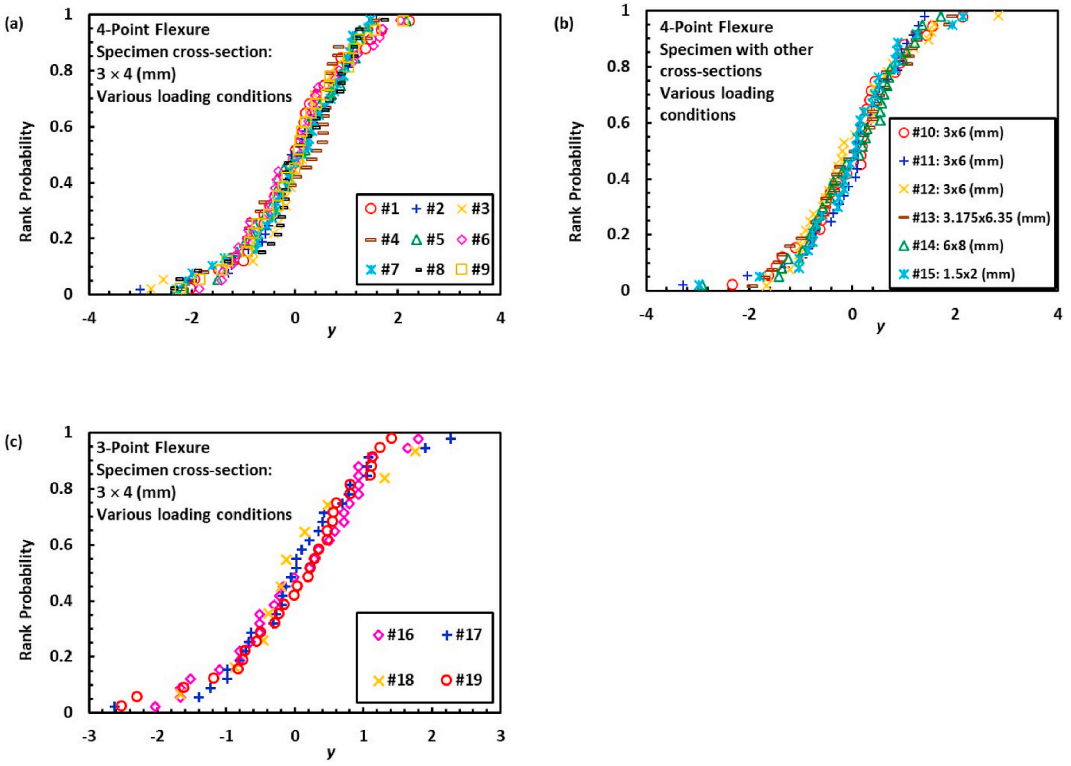

Fig. 8. Standardized representation of strength data in four-point flexure of prismatic beams with cross section size of 3 mm × 4 mm (a), and other cross section sizes (b), and in three-point flexure (c).

(1). Feasibility to estimate Weibull modulus m_0 as an approximation to m_u;
(2). Estimation of m_0 from multiple data sets of same specimens under same loading modes but with different setups and loading rates;
(3). Estimation of m_0 from multiple data sets of different sized specimens under same loading modes but with different setups and loading rates;
(4). Estimation of m_0 from multiple data sets of same or different sized specimens under different loading modes.

4.1. Weibull modulus estimation from a single data set of alumina

This example is intended to examine whether the estimated m_0 is a close approximation to m_u. In other words, it is to examine whether it is acceptable to ignore the effect of the ratio $\sigma_{L,u}/\sigma_N$ on the coefficient k. Gorjan and Ambrožič [3] reported a statistical evaluation of 5100 experimental values of flexural strength of alumina ceramics in a series of four point bending tests. Refer to Fig. 1, the specimen sizes are: $2L = 40\ mm$, $b = 4\ mm$, $2d = 3\ mm$, the inner loading span is $2l = 20\ mm$. In total, 5100 experimental values of flexural strength were measured, with the minimum of 137 MPa, maximum of 400 MPa, average of 290 MPa, and standard deviation of 37.5 MPa. A semi-analytical solution to the cumulative failure probability for a four-point flexural strength test was proposed in Ref. [5] as below,

$$P = 1 - exp\left[-\frac{V}{4(m_u+1)V_0}\left(1-\frac{\sigma_{L,u}}{\sigma_N}\right)\left(\frac{\sigma_N-\sigma_{L,u}}{\sigma_u}\right)^{m_u}\right] \tag{43}$$

or

$$\frac{1}{\left[V/4\left(1-\sigma_{L,u}/\sigma_N\right)\right]} Ln\left(\frac{1}{1-P}\right) = \frac{1}{(m_u+1)V_0}\left(\frac{\sigma_N-\sigma_{L,u}}{\sigma_u}\right)^{m_u} \tag{44}$$

The master curve Equation (44) was used to estimate Weibull parameters ($\sigma_{L,u}$, σ_u, m_u) by least square method, as summarized in Table 1. Now Equation (36) is called in to estimate the Weibull parameters ($\sigma_{L,0}$, σ_0, m_0). The result is shown in Fig. 6 (a) and summarized in Table 1. The estimation leads to $\widehat{m}_0 = 7.03$, which is very close to $\widehat{m}_u = 7.17$ estimated by Equation (44) in Ref. [5]. It suggests that the standardized ordinary Weibull distribution can be used to closely estimate Weibull modulus $\widehat{m}_u$. In addition, the estimation also obtains $\widehat{\sigma}_0 = 239.39\ MPa$ and $\widehat{\sigma}_{L,0} = 66.57\ MPa$, versus $\widehat{\sigma}_u = 164.73\ MPa$ and $\widehat{\sigma}_{L,u} = 55\ MPa$ by Equation (44) in [5]. Fig. 6 also compares the predicted cumulative failure probability by both methods against the experimental result in logarithmic scale **(b)**.

4.2. Weibull modulus estimation from multiple data sets of alumina in uniaxial flexure

The example shown in Section 4.1 involves a single large data set. This section will deal with multiple data sets measured from same or different sized specimens under various conditions including loading mode, loading span, and support span. The strength data are taken from the publicly released final report [18] from the U.S. Army Materials Technology Laboratory for a mechanical testing round robin exercise performed under the auspices of The Technical Cooperation Program (TTCP), a collaboration between the defense establishments of Australia, Canada, New Zealand, the United Kingdom, and the Unites States. Flexural strength at room temperature was measured for a sintered alumina (Al_2O_3) and a reaction-bonded silicon nitride (RBSN). The report reported over 1000 strength data in tables, making it a very valuable database for this study. The project aimed to determine if accurate and consistent results could be obtained in different laboratories using various test procedures in accordance with the U.S. Army MIL-STD-1942 standard for flexure testing of advanced ceramics. Both 3- and 4-point flexures were performed in this round robin, with a variety of specimen sizes on standard or customary fixtures at various loading

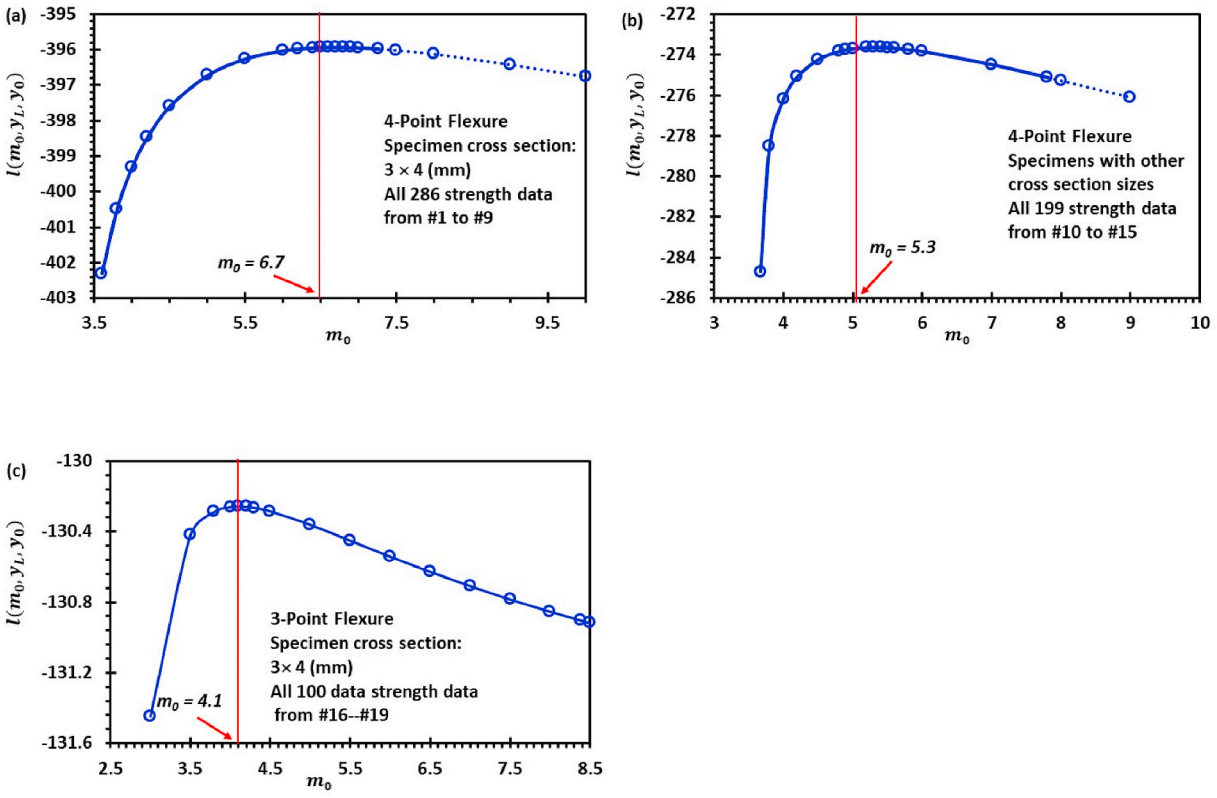

Fig. 9. Variation of log-likelihood function $l(m_0, y_{L,0}, y_0)$ with m_0 for four-point flexure of prismatic beams with cross section size of 3 mm × 4 mm (a), and other cross section sizes (b), and for three-point flexure (c).

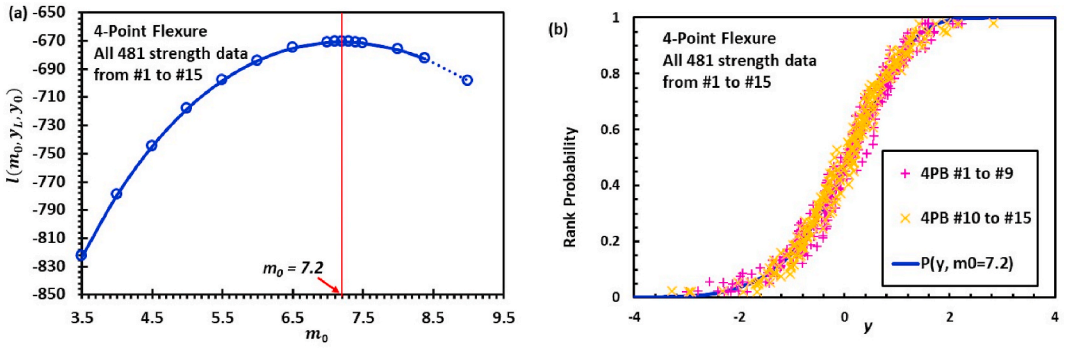

Fig. 10. Analysis of all 4-point flexural strength data from #1 to #15: Variation of log-likelihood function $l(m_0, y_{L,0}, y_0)$ with m_0 (a) and standardized representation (b).

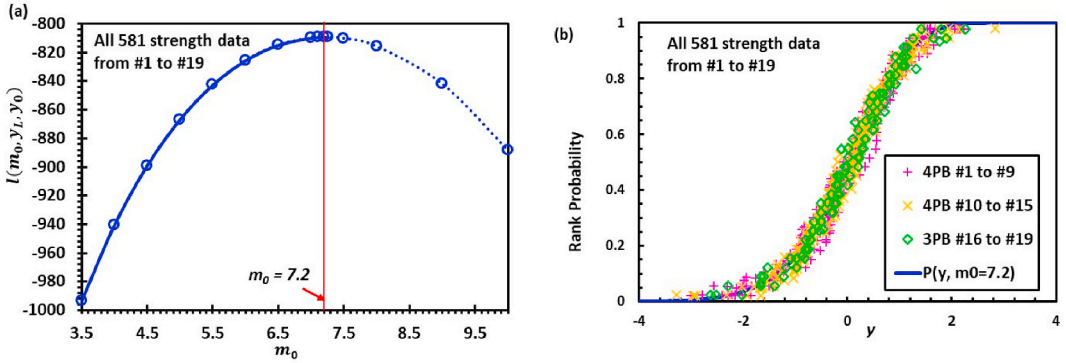

Fig. 11. Analysis of all flexural strength data from #1 to #19: Variation of log-likelihood function $l(m_0, y_{L,0}, y_0)$ with m_0 (a) and standardized representation (b).

Table 3
Summary of flexural experiments of reaction-bonded silicon nitride (RBSN) ceramics.

Data set #	Loading Mode	Specimen Cross-Section Size (mm)	Fixture, Support Span 2L, Loading Span 2*l* (mm)	Loading Rate, mm/min	Number of Specimens	Average Strength, MPa	Standard Deviation, MPa	Laboratory & Operator
1	4PB	3 × 4	MIL STD B Fixture	0.5	30	237	13	MTL (Quinn)
2			$2L = 40\ mm; 2l = 20\ mm$		30	234	12	ORF (Sullivan)
3					30	246	13	NPL (Morrell)
4				2.0	30	274	29	ARE (Godfrey)
5				Unreported	30	230	13	IITRI (for AFWAL)
6			IITRI Modified Fixture $2L = 40\ mm; 2l = 20\ mm$	Unreported	30	229	30.3	IITRI (for AFWAL)
7			NPL Fixture $2L = 40\ mm; 2l = 20\ mm$	0.5	30	237	17	NPL (Morrell)
8			ARE Fixture $2L = 40\ mm; 2l = 19.05\ mm$	2.0	30	263	28	ARE (Godfrey)
9			MIL STD B Fixture	0.5	30	231	22	NPL (Morrell)
10			$2L = 40\ mm; 2l = 20\ mm$ Specimen surface machined		29	248	17	MTL (Quinn)
11	3PB	3 × 4	MIL STD B Fixture		30	267	13	MTL (Quinn)
12			$2L = 40\ mm$	2.0	10	271	13	ARE (Godfrey)
13			ARE Fixture $2L = 40\ mm$	2.0	30	265	24	ARE (Godfrey)
14		4.5 × 4.5	ARE Fixture	2.0	33	292	26	ARE (Godfrey)
15			$2L = 40\ mm$	2.0	33	278	23	ARE (Godfrey)

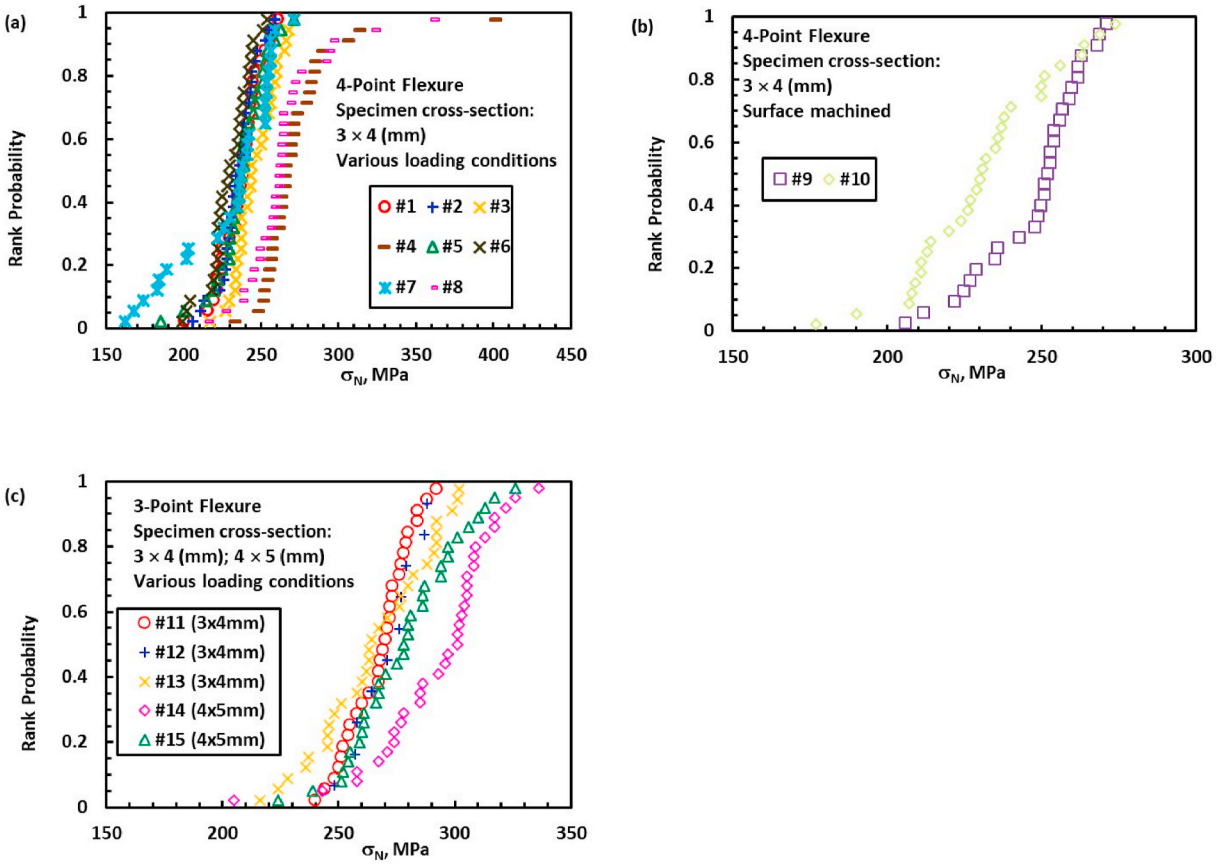

Fig. 12. Experimental strength data [18] of reaction bonded silicon nitride (RBSN) measured by four-point flexure of prismatic beams with cross section size of 3 mm × 4 mm without surface machined (a) and with surface machined (b), and by three-point flexure of prismatic beams with cross section size of 3 mm × 4 mm (c).

rates and ambient room temperature conditions. The two-parameter ordinary Weibull distribution was adopted for statistical analysis. Table 2 summarizes the experimental design and the mean and the standard deviation of strength data of Al_2O_3 in each group. Fig. 7 shows the strength data measured by four-point flexure of prismatic beams with cross section size of 3 mm × 4 mm (a), and other cross section sizes (b), and by three-point flexure of prismatic beams with cross section size of 3 mm × 4 mm (c), respectively.

Fig. 8 shows the corresponding standardized representations of strength data in sequence. In each case, all the standardized strength

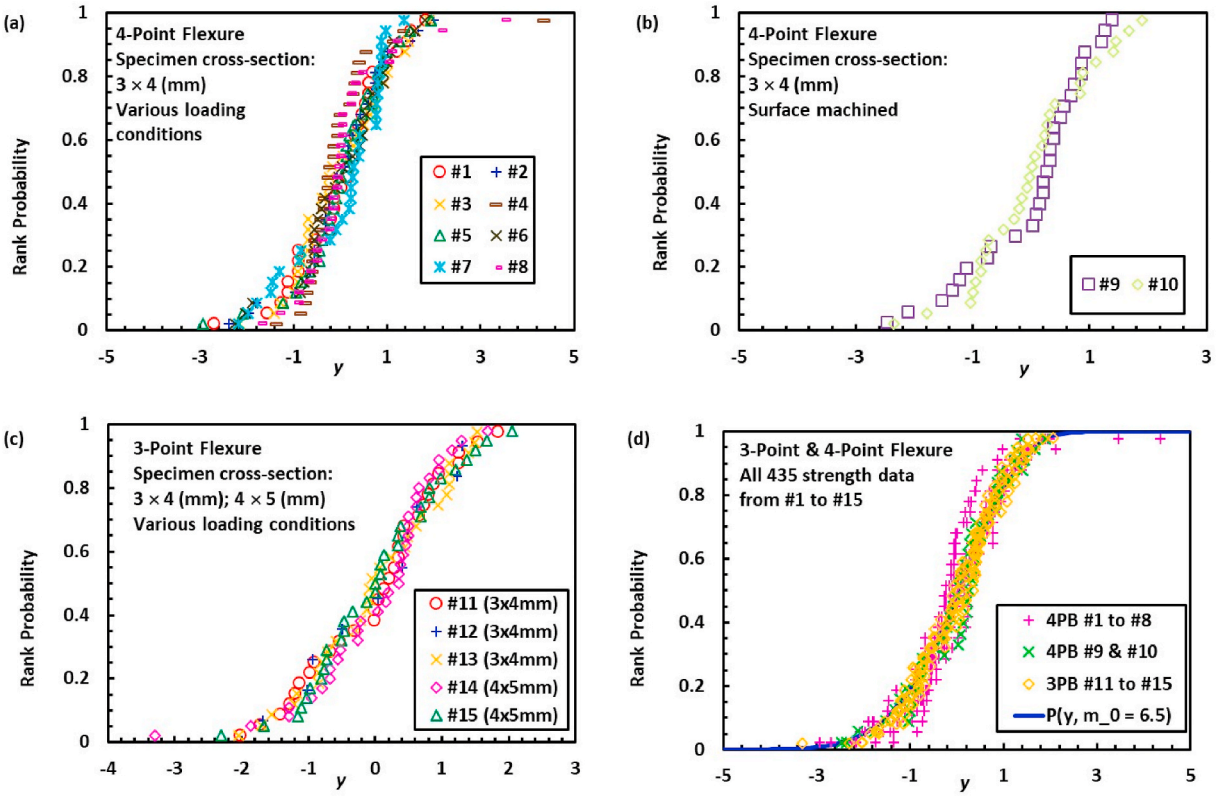

Fig. 13. Standardized representation of strength data in four-point flexure without surface machined (a) and with surface machined (b), in three-point flexure (c), and with all data sets combined (d).

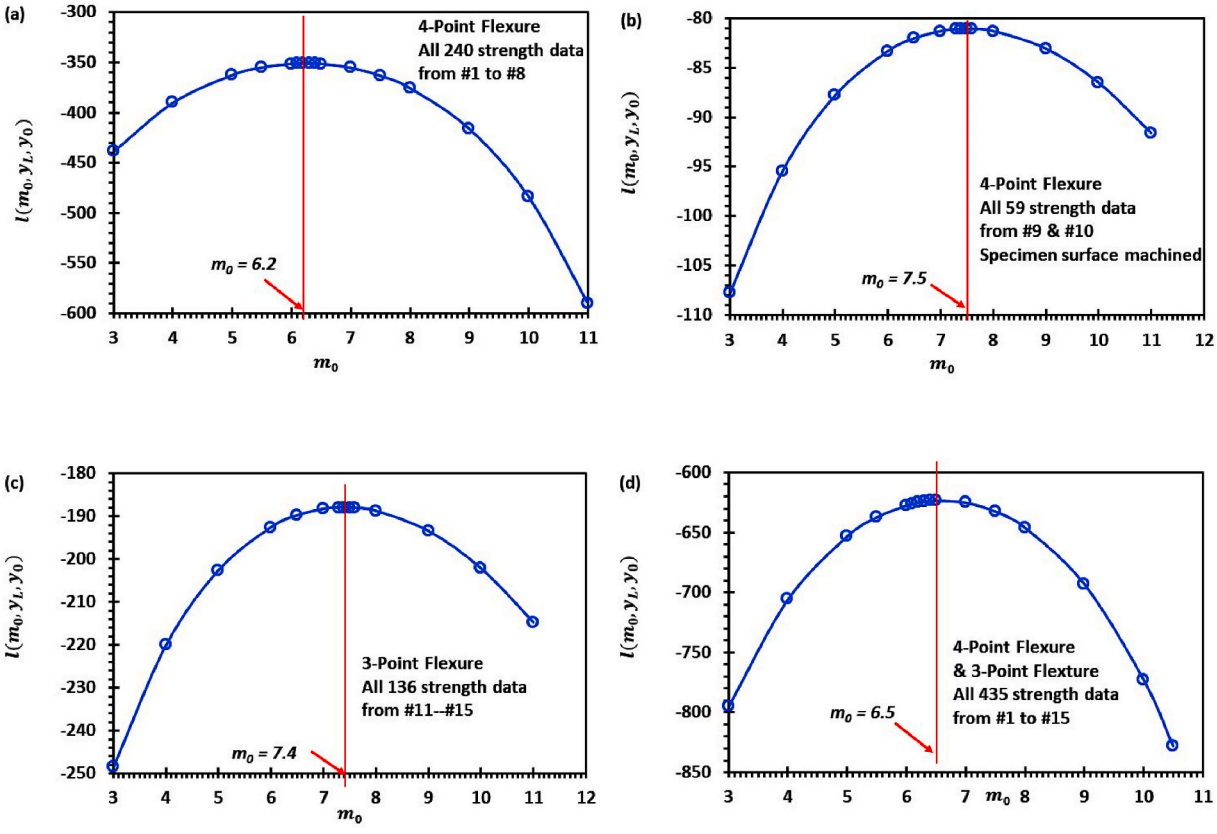

Fig. 14. Maximum likelihood estimation of Weibull modulus with different data sets.

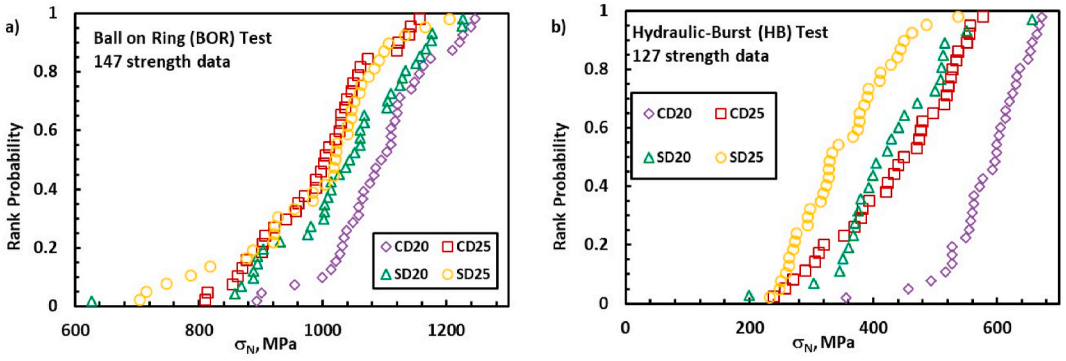

Fig. 15. Experimental strength data of alumina [19] in the ball-on-ring (BOR) test (a) and the hydraulic-burst (HB) test (b).

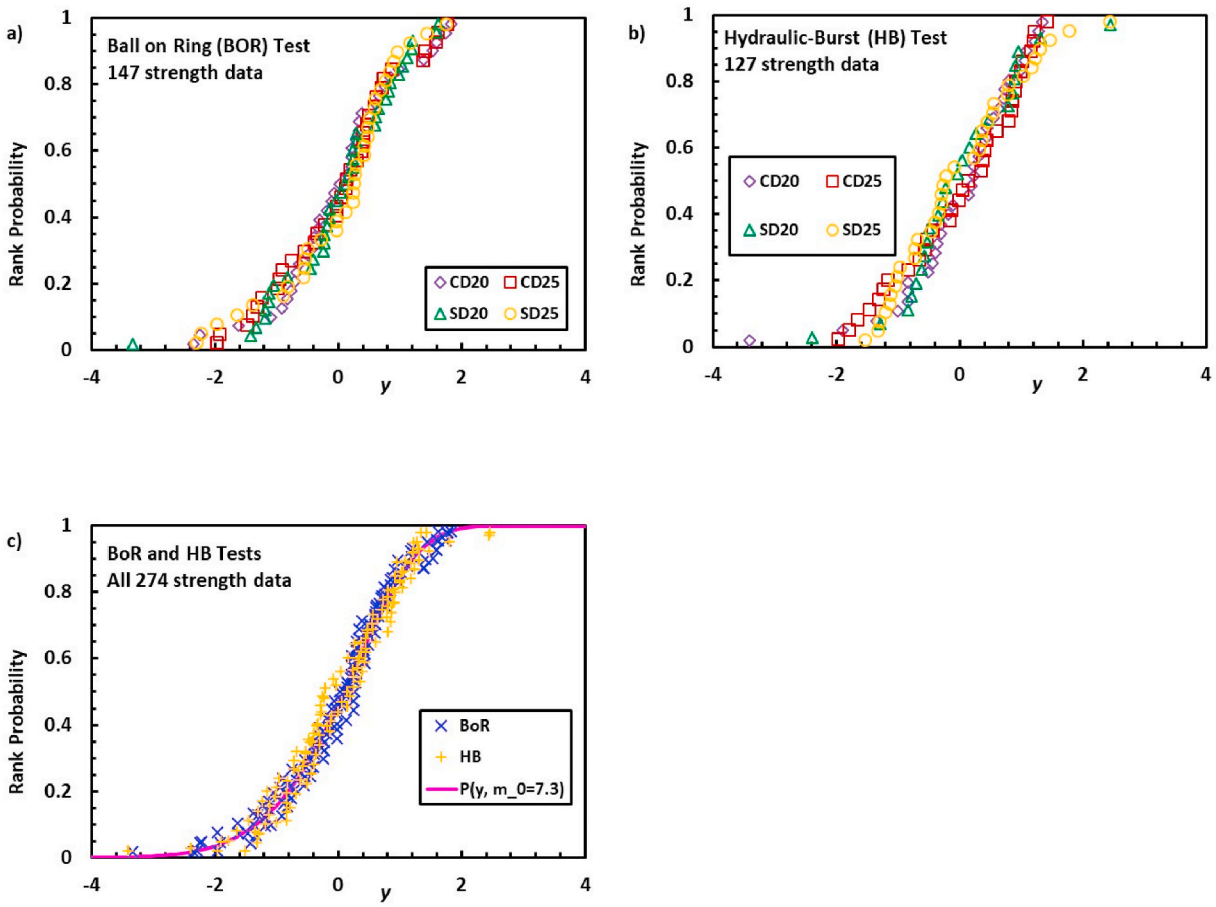

Fig. 16. Standardized data sets for BOR strength only (a), HB strength data only (b), and BOR + HB combined strength data (c).

distribution fall onto a master curve. For each case, the maximum likelihood method is applied to estimate Weibull modulus m_0 as shown in Fig. 9.

The data sets from #1 to #15 for all 4-point flexure tests can be also combined for standardization and maximum likelihood estimation, as shown in Fig. 10. Finally, we can also combine all data sets from #1 to #19 for standardization and maximum likelihood estimation, as show in Fig. 11. All data sets fall onto a single master curve. The small difference in the estimated values of Weibull modulus (4.2–7.2) based on different number of data sets reflects the sample size effect.

4.3. Weibull modulus estimation from multiple data sets of RBSN in uniaxial flexure

The strength data of reaction-bonded silicon nitride (RBSN) used are also taken from Refs. [18]. Table 3 and Fig. 12 summarize the experimental results. Fig. 13 shows the standardized representation of the data sets. It confirms the validity of using the standardized Weibull distribution to synchronize all experimental results. Particularly, on Fig. 13, data sets #9 and #10 from the surface-machined specimens agree well to other data sets from specimens not surface-machined. This supports the conclusion from fractographical analysis that strength-limiting flaws are volume distributed for both alumina and RBSN. Fig. 14 presents the results of maximum likelihood estimation with different combinations of data sets. The estimated Weibull modulus falls in a narrow range of

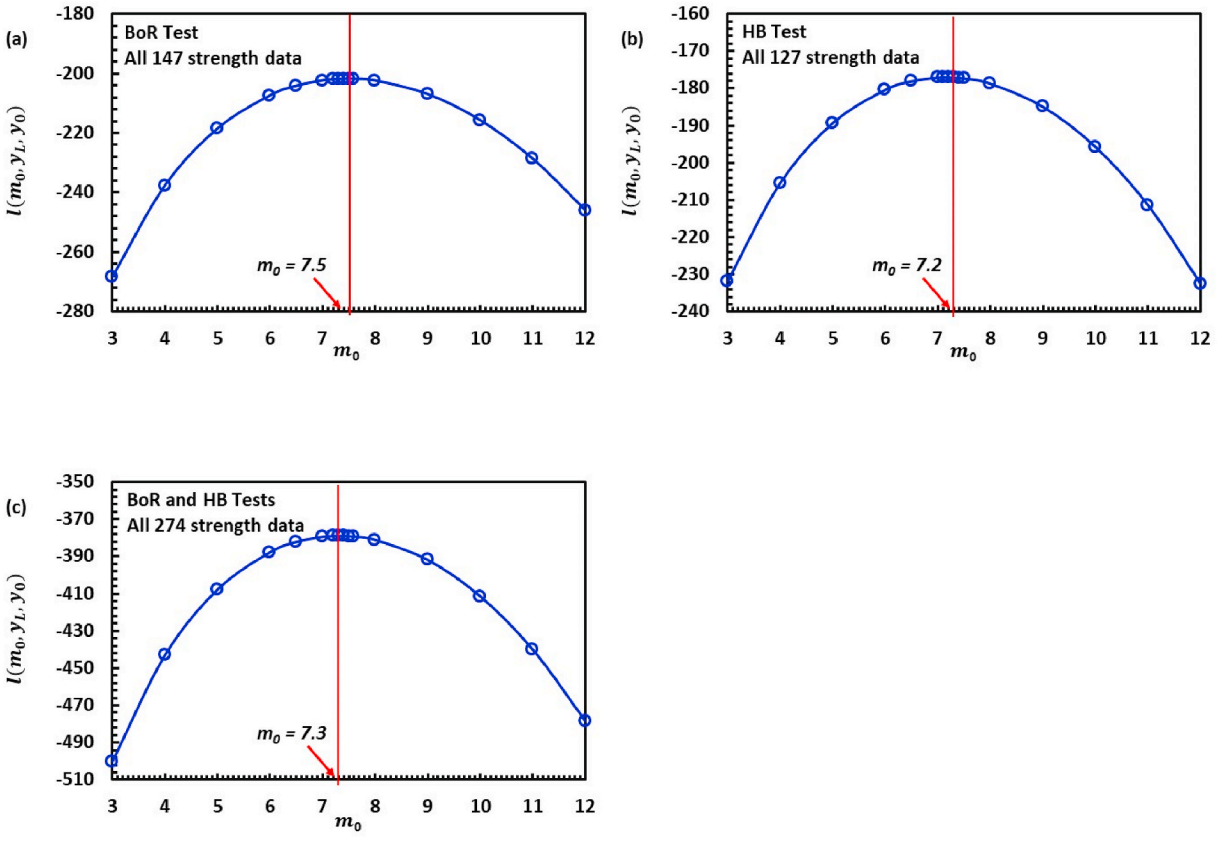

Fig. 17. Maximum likelihood estimation of Weibull modulus with different data sets.

6.2 to 7.5.

4.4. Weibull modulus estimation from multiple data sets of alumina in biaxial flexure

Simpatico et al. [19] measured the biaxial flexural strength of polycrystalline Al_2O_3 tape-cast specimens using the hydraulic-burst (HB) test and the ball-on-ring (BOR) test. In the HB test, hydraulic pressure is applied via a neoprene diaphragm to one side of a specimen that is resting against a support ring. Therefore, the HB test eliminates the very-steep stress gradient which occurs in the BOR test and results in a more uniform stress distribution over the disk. Both square and circular shaped discs, in two different sizes, were tested. The nominal specimen thickness is 0.635 mm. The square discs have edge lengths of 20 and 25 mm and are designated as SD20 and SD25. The circular discs have diameters of 20 and 25 mm and are designated as CD20 and CD25. The stressing rates for the BOR and HB tests were approximately equal. In the BOR setup, load was applied using a 10 mm diameter tungsten carbide ball. The support rings were 16 and 20 mm in diameter for the 20 mm and 25 mm diameter specimens, respectively. The load was applied with a crosshead speed of 0.254 mm/min. The loading rate was ~15 and 10 MPa/s (maximum stress) for the 20 mm and 25 mm specimens, respectively. In the HB setup, the loading rate was 14 and 20 MPa/s (maximum stress) for the 20 mm and 25 mm specimens, respectively. Fig. 15 show the experimental strength data of alumina [19]. Fig. 16 presents the standardized format of the data sets for BOR strength only (a), HB strength data only (b), and BOR + HB combined strength data (c). The results suggest that strength data obtained from two different shaped, different sized specimens on both types of biaxial flexure tests follow a same standardized Weibull distribution. Fig. 17 shows the maximum likelihood estimation of Weibull modulus with different data sets. The estimated Weibull modulus falls in a very narrow range of 7.2–7.5.

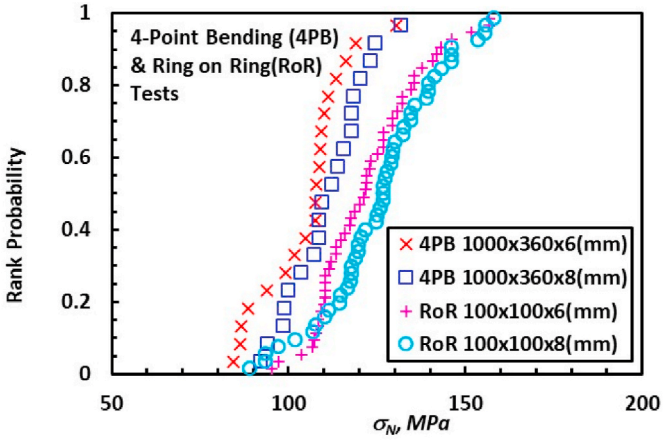

Fig. 18. Experimental strength data of glass-ceramic [20] in the four-point bending (4PB) and the ring-on-ring (RoR) test.

4.5. Weibull modulus estimation from multiple data sets of glass-ceramic in uniaxial and biaxial flexures

The standardized distribution of ceramic strength in either uniaxial or biaxial flexure tests supports the assumption that the coefficient k in Equation (5) is insensitive to $\sigma_{L,u}/\sigma_N$ but still varies with specimen geometry and loading mode, which is the premise for applying the standardized ordinary Weibull distribution for Weibull modulus estimation. This section considers a more complicated scenario by combining

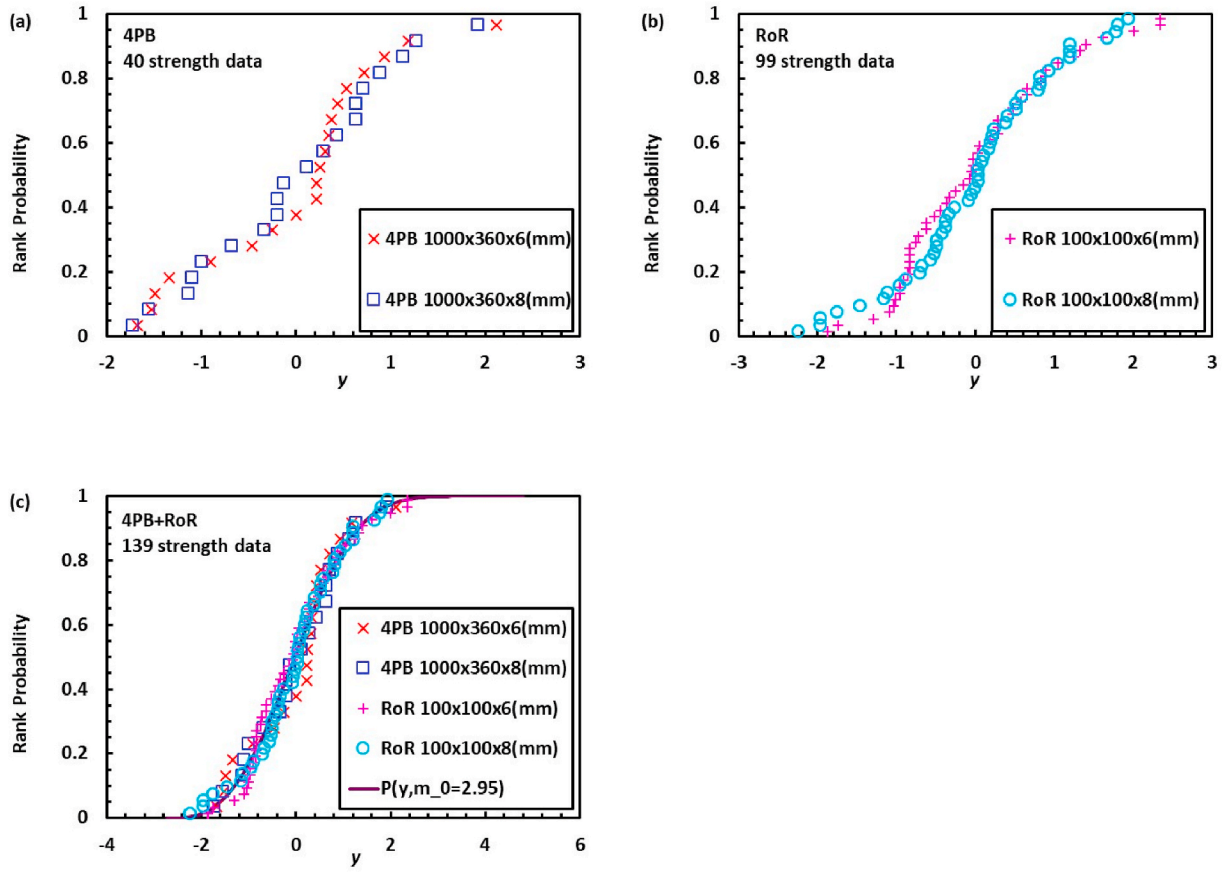

Fig. 19. Standardized representation of the data sets for **(a)**. 4PB strength only, **(b).** RoR strength data only, and **(c).** 4PB + RoR combined strength data.

strength data sets from uniaxial flexure and biaxial flexure. Collini and Carfagni [20] reported strength data of a commercial glass-ceramic measured in four-point bending (4PB) and ring-on-ring (RoR) biaxial flexure. The nominal specimen thickness is 0.635 mm. The 1100 × 360 (mm) rectangular panels were used for the four-point flexure test. The 100 × 100 (mm) tiles were used for the RoR test. For each type of test, two different specimen thicknesses namely, 6 mm and 8 mm, were used. Fig. 18 show the experimental strength data [20]. Fig. 19 presents the standardized distribution of the data sets for 4PB strength only (a), RoR strength data only (b), and 4PB + RoR combined strength data (c). The results suggest that strength data obtained from two different shaped, different sized specimens on uniaxial and biaxial flexure tests follow a same standardized Weibull distribution. Fig. 20 (a), (b), and (c) show the maximum likelihood estimation of Weibull modulus with 2 data sets of 4PB or RoR specimens and all 4 data sets for 4PB and RoR specimens. All the estimations reached $\widehat{m}_0 = 2.9$. To get a preliminary sense of sample size effect on parameter estimation, Fig. 20 (d) shows the maximum likelihood estimation of Weibull modulus with each set of 20 data for 4PB specimens, respectively. The estimation yielded $\widehat{m}_0 = 3.2$ for 6mm thick 4PB specimens and $\widehat{m}_0 = 2.7$ for 8mm thick 4PB specimens. Both are fairly close to $\widehat{m}_0 = 2.95$ from all 4 data sets.

4.6. Weibull modulus estimation from multiple data sets of alumina in flexure of plane and sharply notched specimens

When a notched or pre-cracked specimen is loaded, complex triaxial stress states occur at the notch or crack tip. Previous studies [14,16] concluded the dependence of Weibull modulus on stress concentration factor K_t. It is interesting to compare the standardized distributions of strength measured on smooth and notched specimens. In Refs. [15,16], the effect of stress concentration factor K_t on flexural strength of three ceramic materials was investigated. The materials are fine-grained alumina with mean grain size of 2.3–3 μm, coarse-grained alumina with mean grain size of 20 μm, and zirconia. Three types of specimens were tested, namely the smooth bars ($K_t = 1$), the notched bars with notch depth of 1 mm and notch radius of 0.8 mm ($K_t = 1.78$), and the notched bars with notch depth of 1 mm and notch radius of 0.05 mm ($K_t = 5.88$). All the specimens had an equal gross cross-section of 3 × 4 (mm) and length of 45 mm and were loaded in 4-point flexure with outer support span of 40 mm and inner loading span of 20 mm. The maximum outer fiber stress in the smooth bars and at the notch root in the notched bars was adopted as nominal stress. Fig. 21 show the experimental strength data [15,16]. Fig. 22 presents the standardized strength distributions of each material. The results suggest that regardless of different stress concentration factors involved, the strength data for each material fall onto one standardized Weibull distribution. Fig. 23 shows the maximum likelihood estimation of Weibull modulus for each material. $\widehat{m}_0 = 3.8, 1.62, 18.1$ were obtained for fine-grained alumina, coarse-grained alumina, and zirconia in sequence. Note that for zirconia, as shown in Fig. 23(c), the logarithmic likelihood function $l(y_L, y_0, m_0)$ monotonously increases with m_0. According to the inequality (42) for the range of m_0, m_0 is determined to be within (1.65, 18.13) for $K_t = 1$,

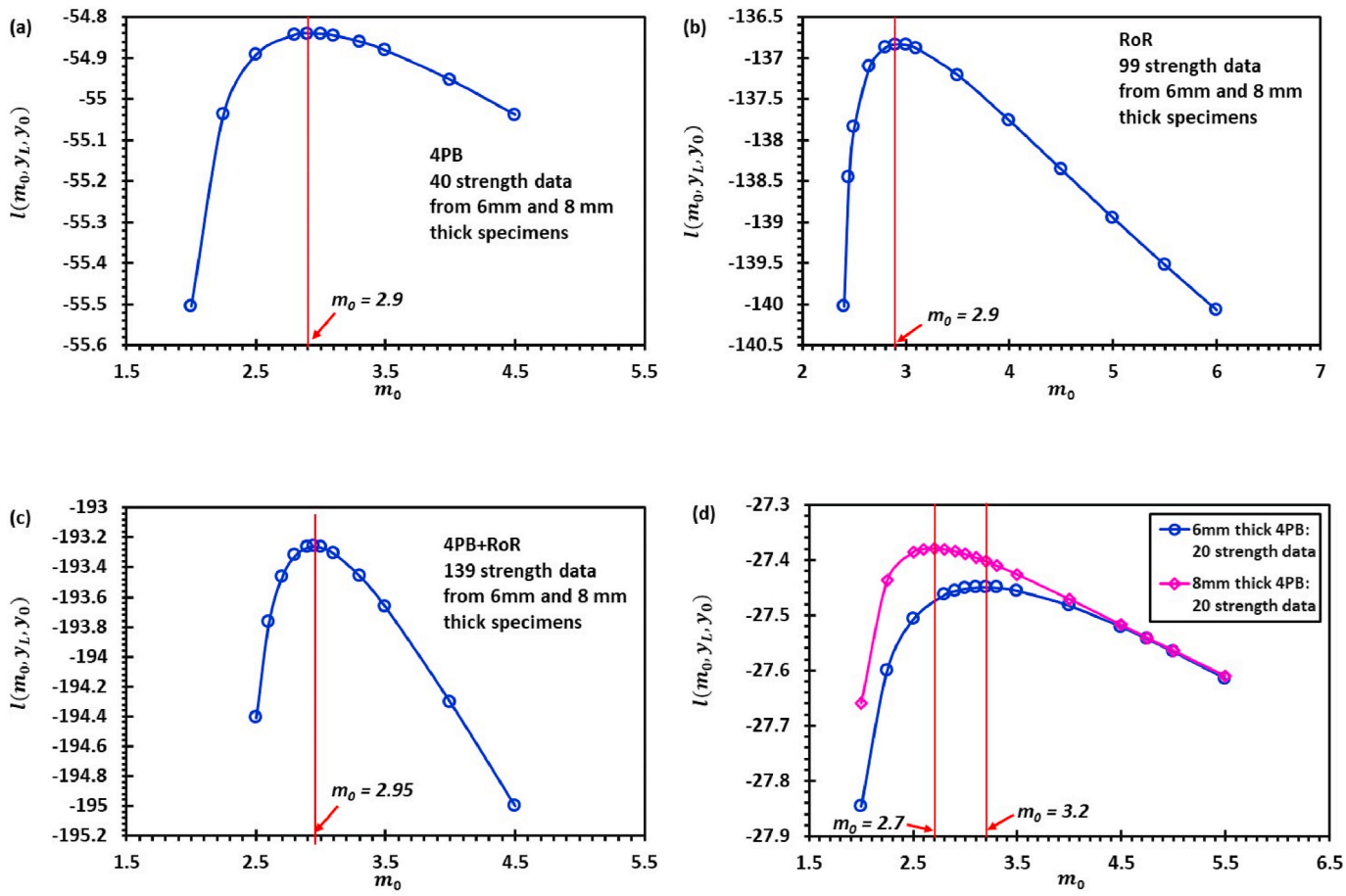

Fig. 20. Maximum likelihood estimation of Weibull modulus with different data sets.

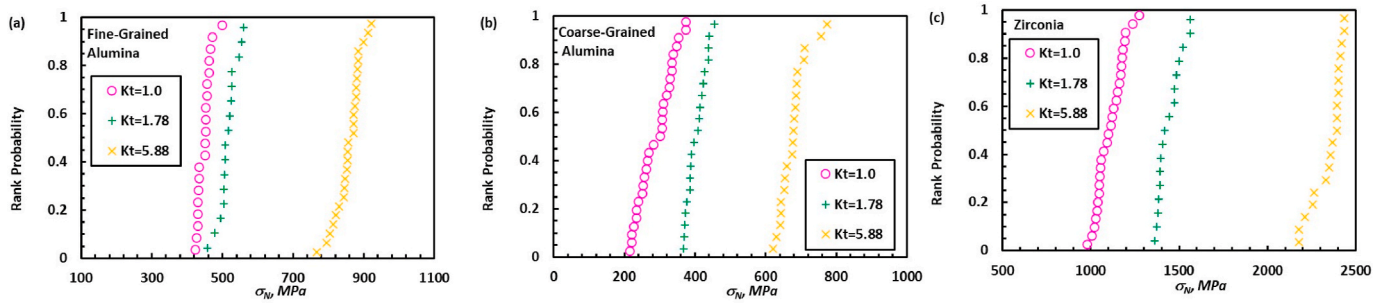

Fig. 21. Experimental strength data of fine-grained alumina [15, 16] **(a)**, coarse-grained alumina [15,16] **(b)**, and zirconia [16] **(c)** in four-point flexure.

(0.98, 26.71) for $K_t = 1.78$, and (1.94, 33.97) for $K_t = 5.88$. Accordingly, $\widehat{m}_0 = 18.1$ is determined for zirconia.

5. Discussions

5.1. The coefficient *k* in equation (5) or (11)

As shown in Section 2, due to the dependence of the coefficient k in Equation (5) or (11) on the ratio $\sigma_{L,u}/\sigma_u$, the Weibull statistical fracture theory does not *strictly* transform into an ordinary Weibull distribution function of the nominal strength. Since we are trying to utilize the ordinary Weibull distribution to estimate Weibull parameters as material property, some approximate treatment must be taken. Specifically, when the coefficient k in Equation (5) or (11) is assumed to be a constant insensitive to the ratio $\sigma_{L,u}/\sigma_u$, transformation of the Weibull statistical fracture theory into an ordinary Weibull distribution of the nominal strength is feasible. Therefore, it is vital to validate the assumption of k as a constant varying with loading mode but insensitive to the ratio $\sigma_{L,u}/\sigma_u$. In principle, the variation of the coefficient k with the ratio $\sigma_{L,u}/\sigma_u$ can be obtained by combining Equation [5] with the cumulative probability as a function of nominal strength for a specific specimen in a specific loading mode. For example, the analytic solutions to the cumulative probability as a function of nominal strength in uniaxial flexure of a prismatic beam with rectangular cross section were developed by Weil and Daniel [21], which demands numerical calculation. The semi-analytical solutions to the same uniaxial flexure problem was provided in [5], such as Equation (43) in Section 4.1 for four-point flexure. Now take the four-point flexure as an example. The combination of Equations (5) and (43) leads to

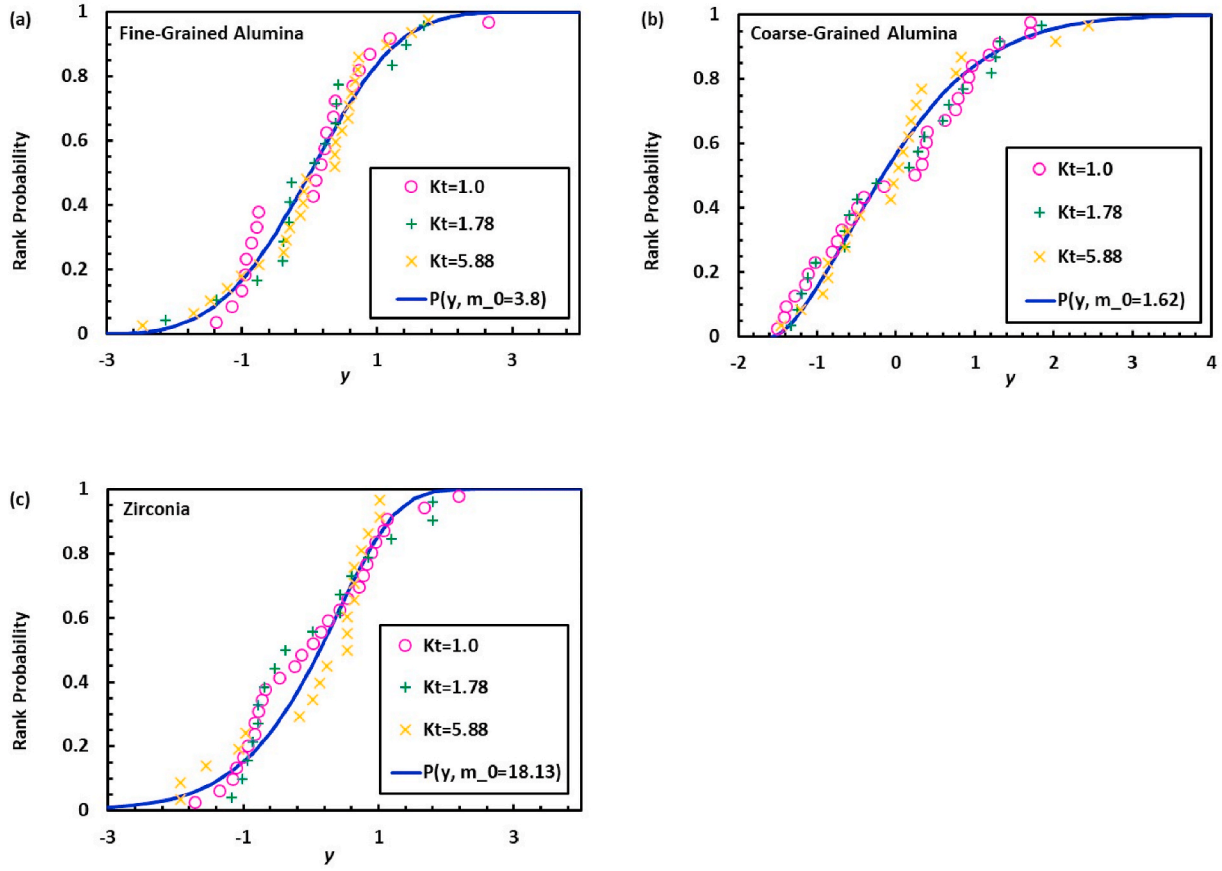

Fig. 22. Standardized representation of strength data of fine-grained alumina **(a)**, coarse-grained alumina **(b)**, and zirconia **(c)**.

$$\left(\frac{k\cdot\sigma_N-\sigma_{L,u}}{\sigma_u}\right)^{m_u}\cdot\frac{V}{V_0}=\frac{V}{4(m_u+1)V_0}\left(1-\frac{\sigma_{L,u}}{\sigma_N}\right)\left(\frac{\sigma_N-\sigma_{L,u}}{\sigma_u}\right)^{m_u} \tag{45}$$

or

$$k=\frac{\sigma_{L,u}}{\sigma_N}+\left[\frac{1}{4(m_u+1)}\left(1-\frac{\sigma_{L,u}}{\sigma_N}\right)\right]^{\frac{1}{m_u}}\left(1-\frac{\sigma_{L,u}}{\sigma_N}\right) \tag{46}$$

Clearly, k monotonously decreases with the increase of $\sigma_N/\ \sigma_{L,u}$ and there is $\sqrt[m_u]{1/[4(m_u+1)]}\le k\le 1$ for $1\le\sigma_N/\sigma_{L,u}<\infty$, as shown in Fig. 24. The range of k is narrow over a large range of $\sigma_N/\ \sigma_{L,u}$ for a given m_u and will be even narrower for engineering ceramics materials since σ_N is far less than ∞, leading to a much narrower range of $\sigma_N/\ \sigma_{L,u}$. For example, for the 5100 flexural strength data of alumina measured by Gorjan and Ambrožič [3] in four-point flexure cited in Section 4.1, the minimum strength is 137 MPa, the maximum strength is 400 MPa, the estimated threshold $\widehat{\sigma}_{L,u}=55\ MPa$ and $\widehat{m}_u=7.17$ in Refs. [5]. Correspondingly, the ratio $\sigma_N/\sigma_{L,u}$ is in the narrow range from 2.49 (= 137/55) to 7.27 (=400/55). Referring to the curve for $m_u=7$ in Fig. 24, there is $0.66\le k\le 0.74$, which indeed supports to approximately treat k as a constant (= 0.70 ± 0.04) independent of the ratio $\sigma_N/\ \sigma_{L,u}$. The Weibull statistical fracture theory-based expressions of cumulative probability as a function of nominal strength are more complex in biaxial and multi-axial loading conditions. Therefore, numerical calculations are needed to investigate the variation of k with the ratio $\sigma_N/\ \sigma_{L,u}$.

5.2. The challenges in calibrating Weibull parameters as material properties

This work introduces the standardized Weibull distribution for Weibull modulus estimation. Once $\widehat{m}_u\approx\widehat{m}_0$ is known, Equations (37) and (38) are called in to obtain $\widehat{\sigma}_0$ and $\widehat{\sigma}_{L,0}$. As shown in Fig. 25, in order to finally obtain $\widehat{\sigma}_u$ and $\widehat{\sigma}_{L,u}$ as material properties, the values of β and k also need to be determined. An approach to estimating β was given in Ref. [1], which demands proportional size scaling of strength with additional experiments to measure strength on different sized specimens of same configuration in a same loading mode. The determination of k would involve numerical calculation. All these will be investigated in future studies.

Here, it is worth mentioning that in an earlier work by Lei [10], the specimen size effect on the strength of alumina in the round robin project [18] is described by Equation (10) with $\beta=0.33$ being determined in Refs. [10]. As shown in Fig. 11, $m_u=7.2$ was estimated for alumina in Section 4.2. Equation (11) is equivalent to:

$$\left\{\frac{1}{\beta(V/V_0)^{\beta}}\cdot\ln\left[\frac{1}{(1-P)}\right]\right\}^{\frac{1}{m_u}}=\frac{k}{\sigma_u}\cdot\sigma_N-\frac{\sigma_{L,u}}{\sigma_u} \tag{47}$$

Therefore, a linear correlation between the compound parameter $\left\{\frac{1}{\beta(V/V_0)^{\beta}}\cdot\ln\left[\frac{1}{(1-P)}\right]\right\}^{\frac{1}{m_u}}$ and nominal strength σ_N is expected. Refer to Table 2, in order to study the size effect on strength of alumina in four-point flexure, the following four data sets measured by the same researcher (Quinn) on different sized specimens are analyzed according

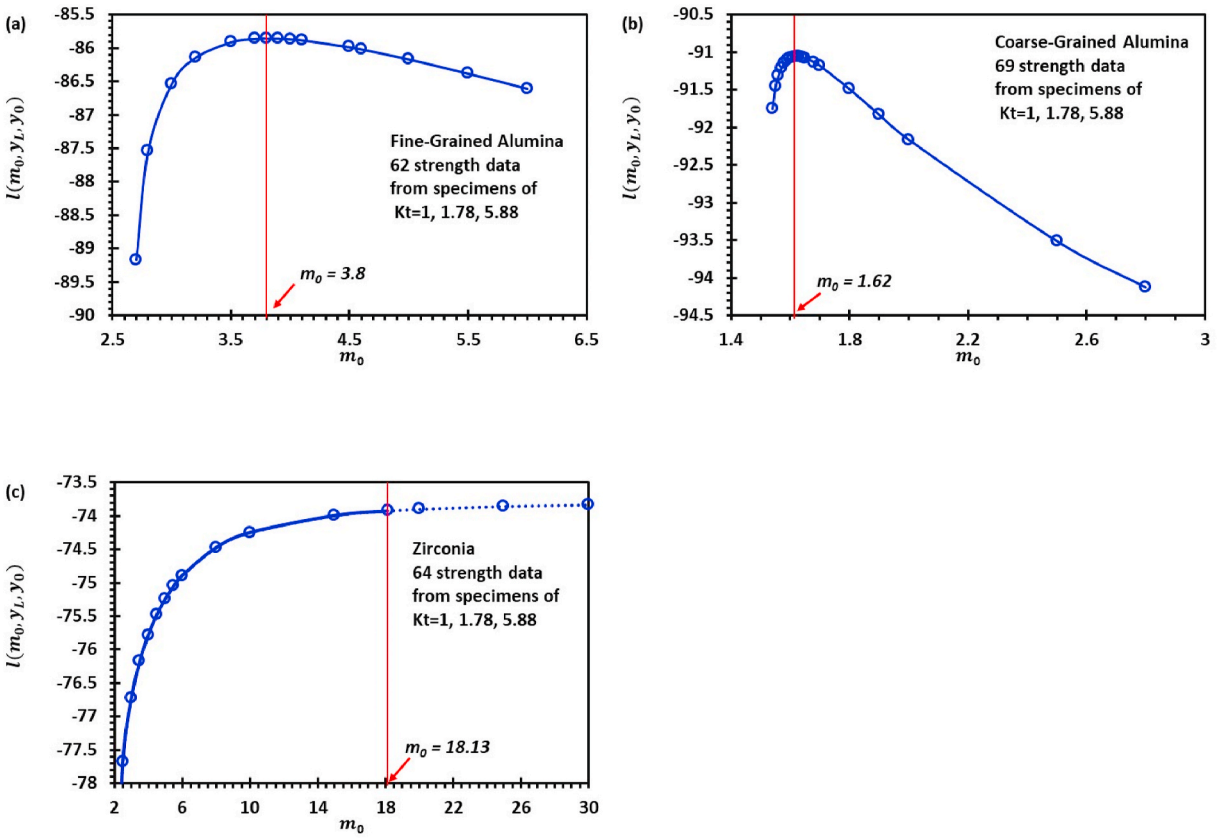

Fig. 23. Maximum likelihood estimation of Weibull modulus of fine-grained alumina **(a)**, coarse-grained alumina **(b)** and zirconia **(c)**.

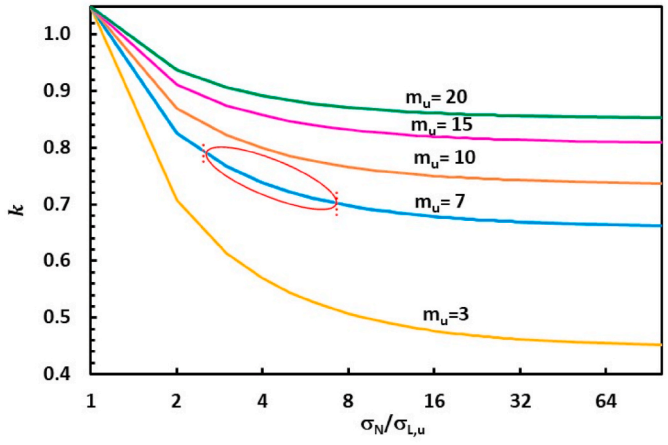

Fig. 24. Variation of k with $\sigma_N/\sigma_{L,u}$ at given m_u in four-point flexure.

to Equation (47), as shown in Fig. 26. The coefficient of determination for the linear correlation between $\left\{\frac{1}{\beta(V/V_0)^\beta}\cdot\ln\left[\frac{1}{(1-P)}\right]\right\}^{\frac{1}{mu}}$ and σ_N is 0.93. Equation (47) is thus validated.

5.3. Effect of sample size on calibration of Weibull parameters

The effect of sample size on the accuracy of distribution parameters is a common concern in calibration of any statistical model. This work is focused on interpreting the basic idea of the proposed approach to calibrating Weibull parameters, with a long-term goal to provide a highly accurate estimation of Weibull modulus and the other two Weibull parameters that enables statistical failure prediction of engineering ceramic components with complex geometries under multiaxial stress states. Accordingly, the adopted data sets of relatively large size (50 or more) are intentionally selected to lower the impact of sample size on calibration. The proposed method has two merits: First, it leaves the argument aside on whether a two- or three-parameter Weibull model should be adopted [5,12,13], and starts with the generic three-parameter Weibull distribution function. If the true threshold strength is zero, the calibrated threshold strength will be either zero or very close to zero. Second, the proposed method allows to calibrate parameters by including multiple sets of data on a same lot of material collected from different experiments in terms of specimen geometry and size as well as loading conditions, so long as the nominally similar types of stress states (predominately either tensile or compressive stresses) are ensured. This is different from the conventional calibration procedures, which only allow to utilize a single data set. Since the proposed approach adopts the sample average and standard deviation as the estimators of population mean and standard deviation to standardize the strength values, the sample size effect on the proposed calibration method should be mainly manifested by the differences between the sample and population values of the mean and the standard deviation. In other words, as a rule of thumb, with the proposed approach, a sample size that ensures a close approximation of the sample average and standard deviation to the population average and standard deviation should also yield a reasonable estimation of Weibull modulus. The sample size is measured by both the number of data sets and the number of data in each data set. As shown in the examples, a single data set is applicable for the proposed approach. In this case, the effect of sample number in one data set on the variation of estimated parameters for a prescribed confidence interval can be investigated in a similar way as adopted for assessing the empirical data fitting approach. In the case of multiple data sets are included, a thorough investigation on the sample size of each data set with a given number of data sets is needed. As

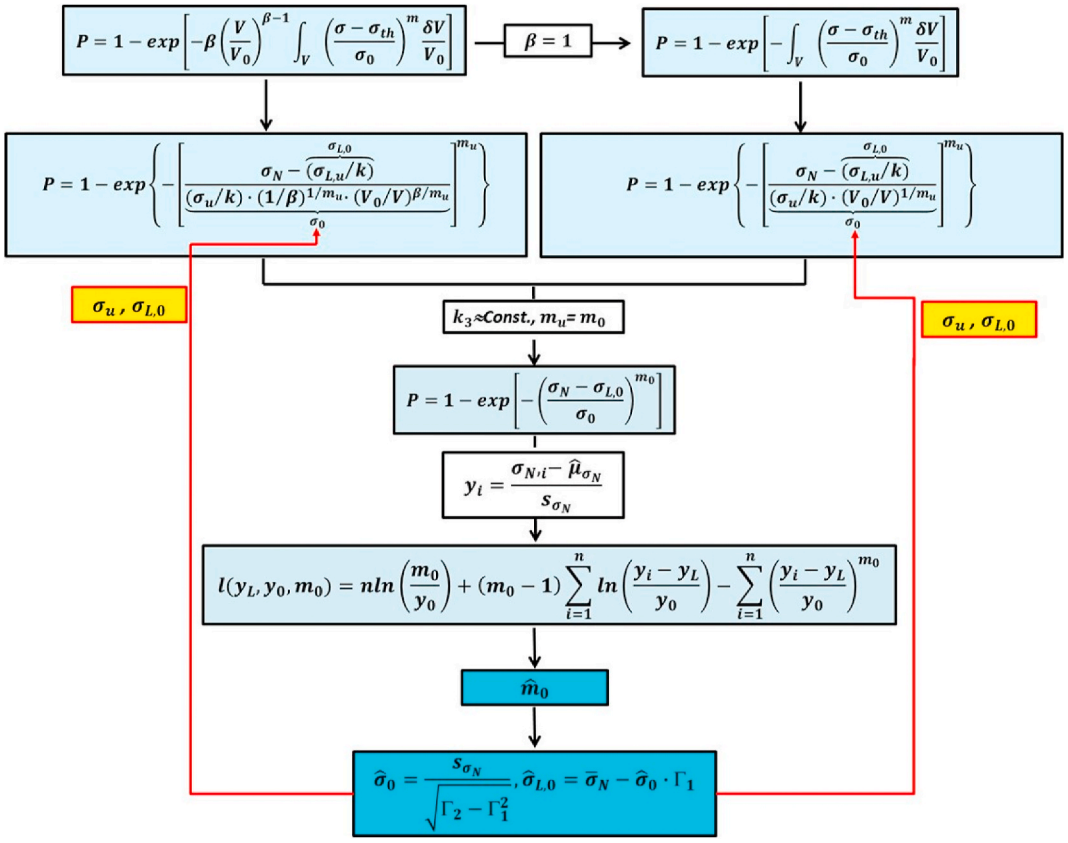

Fig. 25. Flow chart to estimate Weibull parameters (m_u, $\sigma_{L,u}, \sigma_u$) as material properties.

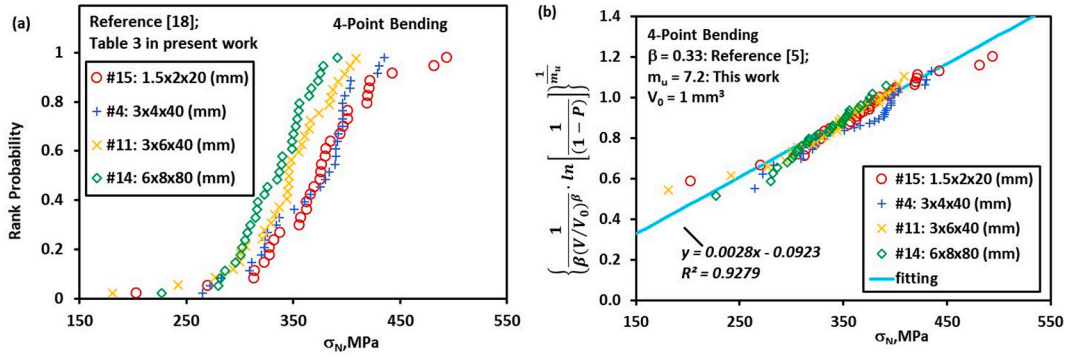

Fig. 26. Experimental strength data of four different sized specimens in four point bending [18] **(a)** and correlation between $\left\{\frac{1}{\beta(V/V_0)^{\beta}}\cdot\ln\left[\frac{1}{(1-P)}\right]\right\}^{\frac{1}{m_u}}$ and σ_N **(b)**.

shown in Fig. 20 (d), with each group of 20 data points for 6mm and 8mm thick 4PB specimens, respectively, the estimated Weibull modulus is within 10% variation ($\hat{m}_0 = 3.2$ and 2.7 from the estimate ($\hat{m}_0 = 2.95$) based on all 139 data points from both 4PB and RoR specimens.

The inequality (42) plays an important role in narrowing down the range of Weibull modulus estimation. It indicates that when the sample size of a data set is relatively small, the proposed approach might be able to yield a pretty close estimation using either a single data set or multiple such data sets. Moreover, Multiple datasets have a clear advantage to improve the accuracy of estimation than a single data set, even when each data set has a small sample size. For the convenience of interpretation, a simple Monte Carlo simulation is conducted as follows: Refer to Equation (2), from a prescribed Weibull distribution with $\sigma_{L,0} = 15$, $\sigma_0 = 80$, and $m_0 = 10$, 3 data sets are randomly generated, each with 15 data points. Fig. 27 (a) shows the three data sets against the prescribed (true) distribution curve. According to inequality (42), the valid range of m_0 for each data set is obtained as below:

Set #1: $A_1 = \{m_0 : 3.00 \le m_0 \le 10.00\}$
Set #2: $A_2 = \{m_0 : 2.78 \le m_0 \le 13.08\}$
Set #3: $A_3 = \{m_0 : 1.77 \le m_0 \le 10.65\}$

When only one data set is adopted to estimate Weibull modulus using the proposed approach, the valid range of m_0 is applied to determine the value of m_0 corresponding to the maximum value of log-likelihood function $l(m_0, y_{L,0}, y_0)$ as the estimate. This is shown in Fig. 27 (b). The single data set based estimation yields $m_0 = 10.00, 13.08, 10.65$ for set#1, #2, and #3 in sequence.

When any two data sets are combined for Weibull modulus estimation, according to the set theory, the valid range of m_0 is the intersection of the two individual sets as below:

Set #1+#2: $A_1 \cap A_2 = \{m_0 : 3.00 \le m_0 \le 10.00\}$
Set #1+#3: $A_1 \cap A_3 = \{m_0 : 3.00 \le m_0 \le 10.00\}$

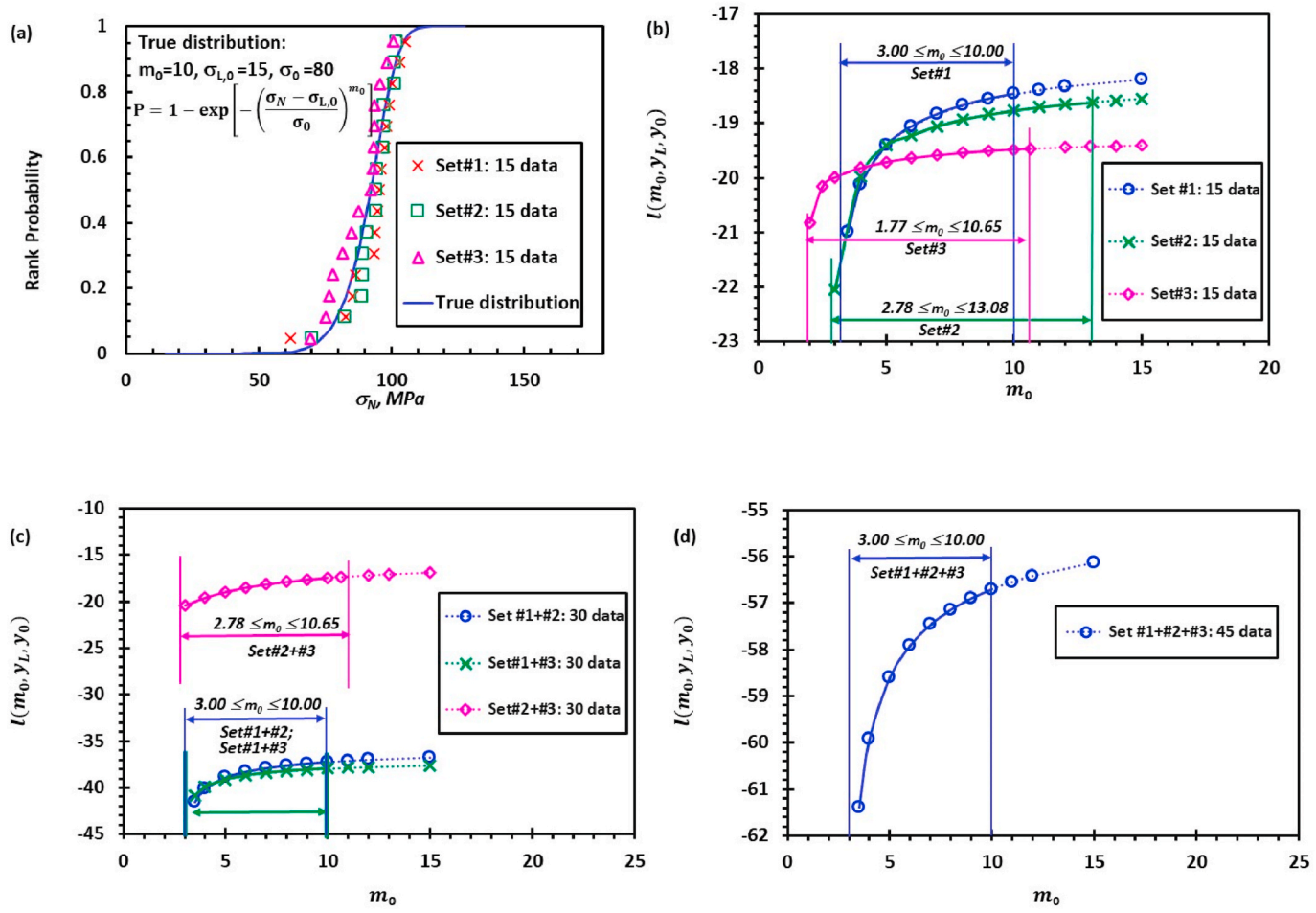

Fig. 27. Weibull modulus estimation based on three randomly generated data sets from a prescribed Weibull distribution: **(a).** 3 sets of 15 randomly generated data and the prescribed distribution; **(b).** Estimation using single data set; **(c).** Estimation using two data sets; **(d).** Estimation using all three data sets.

Set #2+#3: $A_2 \cap A_3 = \{m_0 : 2.78 \le m_0 \le 10.65\}$

where the symbol $\cap$ denotes the operation of intersection of two sets.

Accordingly, the results of estimation are reported in Fig. 27 (c). The two data sets based estimation yields $m_0 = 10.00,\ 10.00,\ 10.65$ for set#1+#2, set#1+#3, and set#2+#3 in sequence.

When all the three data sets are combined for Weibull modulus estimation, according to the set theory, the valid range of m_0 is the intersection of all the three individual sets as below:

Set #1+#2+#3: $A_1 \cap A_2 \cap A_3 = \{m_0 : 3.00 \le m_0 \le 10.00\}$

As shown in Fig. 27 (d), The combination of three data sets yields estimation as $m_0 = 10.00$.

While this example may indicate some potential advantage of the proposed approach in terms of using one or multiple data sets of sample size in each set as small as 15, it is not sufficient to make a conclusion for now. In order to quantitatively assess the bias of each estimated parameter as a function of sample size, the Monte Carlo simulation method is expected to be a useful tool to comprehensively understand the effects of sample size in a data set and the number of data sets. With each given sample size, over ten thousand times of numerical simulations are to be run to gain statistically meaningful conclusions. This will be studied as a separate topic.

6. Summary and conclusions

The two-parameter Weibull statistical fracture theory is widely adopted for ceramic strength prediction due to its simplicity. But it suffers from the specimen geometry (configuration and size) and loading mode dependence of estimated Weibull modulus. It also lacks consensus on zero-valued threshold of strength. The ordinary Weibull distribution works well for fitting a single data set. But the estimated Weibull parameters are not material properties. In recognition of the great challenges to estimate in one effort all Weibull parameters as material properties in the Weibull statistical fracture theory, the work introduces the standardized Weibull distribution to first estimate Weibull modulus. Specifically.

(1) According to the mean value theorem for integrals, the Weibull statistical fracture theory is transformed into the ordinary Weibull distribution under certain assumptions.
(2) The ordinary Weibull distribution is standardized for Weibull modulus estimation.
(3) The maximum likelihood method for the standardized Weibull distribution is introduced. This method allows to combine multiple strength data sets for Weibull modulus estimation. It is a feasible way to estimate Weibull modulus as truly a material property independent of specimen geometry and loading mode.
(4) Extensive case studies of ceramic strength data sets from literature are conducted. They show that for either uniaxial flexure only, biaxial flexure only, the combination of uniaxial and biaxial flexures, or the combination of smooth and notched specimens, all the standardized strength data fall on a master curve uniquely defined by Weibull modulus. This validates the idea of utilizing the standardized Weibull distribution for Weibull modulus estimation.
(5) The inequality (42) defines the valid range of Weibull modulus. It plays an important role in narrowing down the estimation effort.

In order to determine both the scale parameter and the threshold strength as material properties in the Weibull statistical fracture theory, it also needs to determine whether the spatial distribution of flaws in the material of interest is uniformly or non-uniformly distributed, i.e. the value of β in Equations (11) and (47). The effect of sample size and number of data sets on estimation accuracy is also yet well understood. These will be the topics for future study.

Author contributions

WSL: Conceptualization, Methodology, Formal analysis, Validation, Writing-Original draft, review & editing, Data curation; **ZY**: Methodology, Data curation, Validation, Investigation, Writing-Review & editing; **PZ**: Methodology, Investigation, Resources, Writing-Review & editing. ***GQ***: Methodology, Validation, Visualization, Writing - Review & editing.

Declaration of competing interest

The authors declare that they have no known competing financial interests or personal relationships that could have appeared to influence the work reported in this paper.

Acknowledgements

The authors are indebted to Dr. Lovro Gorjan of Jožef Stefan Institute, Ljubljana, Slovenia, for generously sharing his large data set of ceramic flexural strength which is cited and analyzed in this study. The reviewers' suggestions on analyzing effect of sample size for a data set and the number of data sets on estimation accuracy are sincerely appreciated. GQ is grateful to the funding of National Natural Science Foundation of China (No.11872364, 11932020) and Chinese Academy of Science (CAS) Pioneer Hundred Talents Program.

Appendix A. On the variation of the coefficient k in Equation (5) with σ_N via $\sigma_{L,u}/\sigma_N$

Refer to Fig. 1 for three-point flexure, the tensile stress distribution follows Equation (6) within the domain defined by (7a, b). Inserting Equation (6) and the domain in Equation (5) leads to

$$P(\sigma_N)=1-\exp\left\{-\frac{V}{V_0\sigma_u^{m_u}}\int_0^{\left(1-\sigma_{L,u}/\sigma_N\right)}d\left(\frac{z}{d}\right)\int_0^{\left[1-\frac{\sigma_{L,u}}{\sigma_N(1-z/d)}\right]}\left[\sigma_N\cdot\left(1-\frac{z}{d}\right)\left(1-\frac{x}{L}\right)-\sigma_{L,u}\right]^{m_u}d\left(\frac{x}{L}\right)\right\} \tag{A1}$$

or

$$P(\sigma_N)=1-\exp\left\{\frac{V}{V_0\sigma_u^{m_u}}\int_0^{\left(1-\frac{\sigma_{L,u}}{\sigma_N}\right)}d\left(\frac{z}{d}\right)\int_0^{\left[1-\frac{\sigma_{L,u}}{\sigma_N(1-z/d)}\right]}\left[\sigma_N\cdot\left(1-\frac{z}{d}\right)\left(1-\frac{x}{L}\right)-\sigma_{L,u}\right]^{m_u}d\left(1-\frac{x}{L}\right)\right\} \tag{A2}$$

where $V=2bLd$ is the half specimen volume in tension.

Due to

$$\int(ax+b)^n dx=\frac{(ax+b)^{n+1}}{(n+1)a}+C \tag{A3}$$

where C is a constant, Equation (A2) reduces to

$$P(\sigma_N)=1-\exp\left\{\frac{v}{v_0\sigma_u^{m_u}}\int_0^{\left(1-\frac{\sigma_{L,u}}{\sigma_N}\right)}\frac{1}{(m_u+1)\sigma_N\cdot\left(1-\frac{z}{d}\right)}\cdot\left[\sigma_N\cdot\left(1-\frac{z}{d}\right)\left(1-\frac{x}{L}\right)-\sigma_{L,u}\right]^{m_u+1}\Bigg|_0^{\left[1-\frac{\sigma_{L,u}}{\sigma_N\left(1-\frac{z}{d}\right)}\right]}d\left(\frac{z}{d}\right)\right\} \tag{A4}$$

There is

$$\left[\sigma_N\cdot\left(1-\frac{z}{d}\right)\left(1-\frac{x}{L}\right)-\sigma_{L,u}\right]^{m_u+1}\Bigg|_0^{\left[1-\frac{\sigma_{L,u}}{\sigma_N\left(1-\frac{z}{d}\right)}\right]}=-\left[\sigma_N\cdot\left(1-\frac{z}{d}\right)-\sigma_{L,u}\right]^{m_u+1} \tag{A5}$$

Hence, Equation (A4) reduces to

$$P(\sigma_N)=1-\exp\left\{\frac{V}{V_0\sigma_u^{m_u}(m_u+1)\sigma_N}\int_0^{\left(1-\frac{\sigma_{L,u}}{\sigma_N}\right)}\frac{1}{\left(1-\frac{z}{d}\right)}\cdot\left[\sigma_N\cdot\left(1-\frac{z}{d}\right)-\sigma_{L,u}\right]^{m_u+1}d\left(1-\frac{z}{d}\right)\right\} \tag{A6}$$

or

$$P(\sigma_N) = 1 - \exp\left\{ \frac{V}{V_0 \sigma_u^{m_u} (m_u + 1)\sigma_N} \int_0^{\left(1-\frac{\sigma_{L,u}}{\sigma_N}\right)} \left[\sigma_N \cdot \left(1 - \frac{z}{d}\right) - \sigma_{L,u}\right]^{m_u+1} d\left[Ln\left(1 - \frac{z}{d}\right)\right] \right\} \tag{A7}$$

Using the method of integration by parts, we get

$$\int_0^{\left(1-\frac{\sigma_{L,u}}{\sigma_N}\right)} \left[\sigma_N \cdot \left(1 - \frac{z}{d}\right) - \sigma_{L,u}\right]^{m_u+1} d\left[Ln\left(1 - \frac{z}{d}\right)\right] = -(m_u + 1)\sigma_N \int_0^{\left(1-\frac{\sigma_{L,u}}{\sigma_N}\right)} \left[Ln\left(1 - \frac{z}{d}\right)\right] \left[\sigma_N \cdot \left(1 - \frac{z}{d}\right) - \sigma_{L,u}\right]^{m_u} d\left(1 - \frac{z}{d}\right) \tag{A8}$$

Therefore, Equation (A7) is rewritten as

$$P(\sigma_N) = 1 - \exp\left\{ -\frac{V}{V_0 \sigma_u^{m_u}} \int_0^{\left(1-\frac{\sigma_{L,u}}{\sigma_N}\right)} \left[Ln\left(1 - \frac{z}{d}\right)\right] \left[\sigma_N \cdot \left(1 - \frac{z}{d}\right) - \sigma_{L,u}\right]^{m_u} d\left(1 - \frac{z}{d}\right) \right\} \tag{A9}$$

According to the second mean value theorem for definite integrals, since $Ln\left(1 - \frac{z}{d}\right)$ is a monotonic function within the domain [0, $(1 - \sigma_{L,u}/\sigma_N)$], we get

$$\int_0^{\left(1-\frac{\sigma_{L,u}}{\sigma_N}\right)} \left[Ln\left(1 - \frac{z}{d}\right)\right] \left[\sigma_N \cdot \left(1 - \frac{z}{d}\right) - \sigma_{L,u}\right]^{m_u} d\left(1 - \frac{z}{d}\right) = Ln(1-0) \int_0^{\xi} \left[\sigma_N \cdot \left(1 - \frac{z}{d}\right) - \sigma_{L,u}\right]^{m_u} d\left(1 - \frac{z}{d}\right) + Ln\left(\frac{\sigma_{L,u}}{\sigma_N}\right) \int_{\xi}^{\left(1-\frac{\sigma_{L,u}}{\sigma_N}\right)} \left[\sigma_N \cdot \left(1 - \frac{z}{d}\right) - \sigma_{L,u}\right]^{m_u} d\left(1 - \frac{z}{d}\right) \tag{A10}$$

or

$$\int_0^{\left(1-\frac{\sigma_{L,u}}{\sigma_N}\right)} \left[Ln\left(1 - \frac{z}{d}\right)\right] \left[\sigma_N \cdot \left(1 - \frac{z}{d}\right) - \sigma_{L,u}\right]^{m_u} d\left(1 - \frac{z}{d}\right) = Ln\left(\frac{\sigma_{L,u}}{\sigma_N}\right) \int_{\xi}^{\left(1-\frac{\sigma_{L,u}}{\sigma_N}\right)} \left[\sigma_N \cdot \left(1 - \frac{z}{d}\right) - \sigma_{L,u}\right]^{m_u} d\left(1 - \frac{z}{d}\right) \tag{A11}$$

where ξ is a constant and $0 \le \xi \le 1 - \frac{\sigma_{L,u}}{\sigma_N}$.

In aid of Equation (3A), we get

$$\int_{\xi}^{\left(1-\frac{\sigma_{L,u}}{\sigma_N}\right)} \left[\sigma_N \cdot \left(1 - \frac{z}{d}\right) - \sigma_{L,u}\right]^{m_u} d\left(1 - \frac{z}{d}\right) = \frac{1}{(m_u + 1)\sigma_N \cdot \left(1 - \frac{z}{d}\right)} \cdot \left[\sigma_N \cdot \left(1 - \frac{z}{d}\right) - \sigma_{L,u}\right]^{m_u+1} \Bigg|_{\xi}^{\left(1-\frac{\sigma_{L,u}}{\sigma_N}\right)} \tag{A12}$$

or

$$\int_{\xi}^{\left(1-\frac{\sigma_{L,u}}{\sigma_N}\right)} \left[\sigma_N \cdot \left(1 - \frac{z}{d}\right) - \sigma_{L,u}\right]^{m_u} d\left(1 - \frac{z}{d}\right) = -\frac{\left[\sigma_N \cdot (1 - \xi) - \sigma_{L,u}\right]^{m_u+1}}{(m_u + 1)\sigma_N \cdot (1 - \xi)} \tag{A13}$$

Equation (A11) thus reduces to

$$\int_0^{\left(1-\frac{\sigma_{L,u}}{\sigma_N}\right)} \left[Ln\left(1 - \frac{z}{d}\right)\right] \left[\sigma_N \cdot \left(1 - \frac{z}{d}\right) - \sigma_{L,u}\right]^{m_u} d\left(1 - \frac{z}{d}\right) = -Ln\left(\frac{\sigma_{L,u}}{\sigma_N}\right) \frac{\left[\sigma_N \cdot (1 - \xi) - \sigma_{L,u}\right]^{m_u+1}}{(m_u + 1)\sigma_N \cdot (1 - \xi)} \tag{A14}$$

Substituting Equation (A14) into (A9) gives

$$P(\sigma_N) = 1 - \exp\left\{ \frac{V}{V_0 \sigma_u^{m_u}} Ln\left(\frac{\sigma_{L,u}}{\sigma_N}\right) \frac{\left[\sigma_N \cdot (1 - \xi) - \sigma_{L,u}\right]^{m_u+1}}{(m_u + 1)\sigma_N \cdot (1 - \xi)} \right\} \tag{A15}$$

Comparing Equation (5) in Section 2 with Equation (A15), we get

$$-\left(k\cdot\sigma_N-\sigma_{L,u}\right)^{m_u}=Ln\left(\frac{\sigma_{L,u}}{\sigma_N}\right)\ \frac{\left[\sigma_N\cdot(1-\xi)-\sigma_{L,u}\right]^{m_u+1}}{(m_u+1)\sigma_N\cdot(1-\xi)} \tag{A16}$$

or

$$k=\frac{\sigma_{L,u}}{\sigma_N}+\left\{Ln\left(\frac{\sigma_N}{\sigma_{L,u}}\right)\ \frac{\left[(1-\xi)-\ \frac{\sigma_{L,u}}{\sigma_N}\right]^{m_u+1}}{(m_u+1)\cdot(1-\xi)}\right\}^{\frac{1}{m_u}} \tag{A17}$$

This proves the dependence of k on v σ_N ia. $\sigma_{L,u}/\sigma_N$ Equation (A17) can be rewritten as Equation (9) in Section 2. {\displaystyle \int _{a}^{b}G(t)\varphi (t)\,dt = G (a^{+})\int _{a}^{x}\varphi (t)\,dt + G (b^{-})\int _{x}^{b}\varphi (t)\,dt.}

References

[1] W.-S. Lei, A generalized weakest-link model for size effect on strength of quasi-brittle materials, J. Mater. Sci. 53 (2018) 1227–1245.
[2] W. Weibull, A statistical distribution function of wide applicability, J. Appl. Mech. 18 (1951) 293–297.
[3] L. Gorjan, M. Ambrožič, Bend strength of alumina ceramics: a comparison of Weibull statistics with other statistics based on very large experimental data set, J. Eur. Ceram. Soc. 32 (2012) 1221–1227.
[4] G. Qian, W.-S. Lei, Z. Yu, F. Berto, Statistical size scaling of breakage strength of irregularly-shaped particles, Theor. Appl. Fract. Mech. 102 (2019) 51–58.
[5] W.-S. Lei, P. Zhang, Z. Yu, G. Qian, Statistics of ceramic strength: use ordinary Weibull distribution function or Weibull statistical fracture theory? Ceram. Int. 46 (2020) 20751–20768.
[6] W. Weibull, A statistical theory of the strength of materials, Ingeniorsvetenskapakademiens Handlinger 151 (1939) 1–45.
[7] W.-S. Lei, A framework for statistical modeling of plastic yielding initiated cleavage fracture of structural steels, Philos. Mag. A 96 (2016) 3586–3631.
[8] S.S. Sanni, W.I.E. Chukwu, An economic order quantity model for items with three-parameter Weibull distribution deterioration, ramp-type demand and shortages, Appl. Math. Model. 37 (2013) 9698–9706.
[9] P. Damos, P. Soulopoulou, Do insect populations die at constant rates as they become older? contrasting demographic failure kinetics with respect to temperature according to the Weibull model", PloS One 10 (2015), e0127328 https://doi.org/10.1371/journal.pone.0127328.
[10] W.-S. Lei, Statistical size scaling of ceramic strength, J. Am. Ceram. Soc. 102 (2019) 90–97.
[11] W.-S. Lei, G. Qian, Z. Yu, F. Berto, Statistical size scaling of compressive strength of quasi-brittle materials incorporating specimen length-to-diameter ratio effect, Theor. Appl. Fract. Mech. 104 (2019) 102345.
[12] J. Malzbender, R.W. Steinbrech, Threshold fracture stress of thin ceramic components, J. Eur. Ceram. Soc. 28 (2008) 247–252.
[13] J. Smart, B.C. Mitchell, S.L. Fok, B.J. Marsden, The effect of the threshold stress on the determination of the Weibull parameters in probabilistic failure analysis, Eng. Fract. Mech. 70 (2003) 2559–2567.
[14] T. Hoshide, J. Murano, R. Kusaba, Effect of specimen geometry on strength in engineering ceramics, Eng. Fract. Mech. 59 (5) (1998) 655–665.
[15] D. Hertel, T. Fett, D. Munz, Strength predictions for notched alumina specimens, J. Eur. Ceram. Soc. 18 (4) (1998) 329–338.
[16] T. Fett, D. Hertel, D. Munz, Strength of notched ceramic bending bars, J. Mater. Sci. Lett. 18 (1999) 289–293.
[17] Wikipedia, Unbiased estimation of standard deviation. https://en.wikipedia.org/wiki/Unbiased_estimation_of_standard_deviation.
[18] G.D. Quinn, Flexure strength of advanced ceramics—a round robin exercise. U.S. Army Materials Technology Laboratory Report, Approved for public release. Available at: http://www.dtic.mil/dtic/tr/fulltext/u2/a212101.pdf, 1989.
[19] A. Simpatico, W.R. Cannon, M.J. Matthewson, Comparison of hydraulic-burst and ball-on ring tests for measuring biaxial strength, J. Am. Ceram. Soc. 82 (1999) 2737–2744.
[20] L. Collini, G.R. Carfagni, Flexural strength of glass–ceramic for structural applications, J. Eur. Ceram. Soc. 34 (11) (2014) 2675–2685.
[21] N.A. Weil, I.M. Daniel, Analysis of fracture probabilities in nonuniformly stressed brittle materials, J. Am. Ceram. Soc. 47 (1964) 268–274.